
Article:
Mohsenian, V. orcid.org/0000-0002-5918-1569, Filizadeh, R. orcid.org/0000-0002-9580-5121, Mariani, S. orcid.org/0000-0001-5111-9800 et al. (1 more author) (2024) Probabilistic assessment of global damage index for steel moment-resisting frames based on local responses. Journal of Earthquake Engineering, 28 (10). pp. 2855-2882. ISSN: 1363-2469

https://doi.org/10.1080/13632469.2024.2312938

Journal of Earthquake Engineering

ISSN: 1363-2469 (Print) 1559-808X (Online) Journal homepage: www.tandfonline.com/journals/ueqe20

Probabilistic Assessment of Global Damage Index for Steel Moment-Resisting Frames Based on Local Responses

Vahid Mohsenian, Reza Filizadeh, Stefano Mariani & Iman Hajirasouliha

To cite this article: Vahid Mohsenian, Reza Filizadeh, Stefano Mariani & Iman Hajirasouliha (2024) Probabilistic Assessment of Global Damage Index for Steel Moment-Resisting Frames Based on Local Responses, Journal of Earthquake Engineering, 28:10, 2855-2882, DOI: 10.1080/13632469.2024.2312938

To link to this article: https://doi.org/10.1080/13632469.2024.2312938

Published online: 05 Feb 2024.

JOURNAL OF EARTHQUAKE ENGINEERING
2024, VOL. 28, NO. 10, 2855–2882
https://doi.org/10.1080/13632469.2024.2312938

Taylor & Francis
Taylor & Francis Group

Probabilistic Assessment of Global Damage Index for Steel Moment-Resisting Frames Based on Local Responses

Vahid Mohsenian [a], Reza Filizadeh [b], Stefano Mariani [c], and Iman Hajirasouliha [d]

[a]Department of Civil Engineering, University of Science and Culture, Tehran, Iran; [b]Department of Civil Engineering, Sharif University of Technology, Tehran, Iran; [c]Department of Civil and Environmental Engineering, Politecnico di Milano, Milano, Italy; [d]Department of Civil and Structural Engineering, The University of Sheffield, Sheffield, UK

ABSTRACT

A new scenario-based method is proposed to determine the performance range of structural systems. The advantage of this method is using inter-storey drift as a damage index, while exploiting local damage indices of the main structural members without the need for detailed analytical models and computationally expensive non-linear dynamic analyses. A new damage function is proposed by linking the local (plastic hinge rotations) and global (inter-storey drifts) damage levels. The accuracy of the proposed function is evaluated and compared with the indices in ASCE41–06, ATC-13, and HAZUS for a set of steel moment-resisting frames subjected to earthquakes of varying intensities.

ARTICLE HISTORY
Received 27 March 2023
Accepted 26 January 2024

KEYWORDS
Global damage index; local damage index; incremental dynamic analysis; fragility analysis; performance level

1. Introduction

The damage state in a structure is usually characterized by a dimensionless index, which defines the local or global reduction of the system's stiffness and strength properties (Krawinkler and Nassar 1992). Since a damage index is a coefficient that proportionally reduces the mechanical features of the structural members, the higher value it takes, the more severe the damage suffered by the structure. According to damage mechanics, the index value is zero in the undamaged state of the structure, and its value can increase to 1 in the event of an overall failure. In general, damage indices can be classified into three general categories as follows:

(1) *Local damage indices* are related to the damage level in a single structural member.
(2) *Intermediate damage indices* define the damage level in a storey of a building or, more generally, in a substructure.
(3) *Global damage indices* measure the damage state in the whole structure and quantify its overall performance. These indices are obtained by mixing all the local damage index values throughout the structure. In most cases the collapse of a storey directly affects the performance of the entire structure, so the formerly mentioned intermediate damage indices can also be considered global damage indicators.

In the literature, various indicators have been proposed to quantify the damage and assess the performance level of structural systems. The damage index proposed by Park et al. (1987), which is based on the displacements and the dissipated energy, is well-known and widely used especially for RC structures. Ghosh et al. (2011) conducted a statistical study on the Park-Ang damage index for different ductility capacities and calibration factor (β) values. They proposed equivalent single-

CONTACT Vahid Mohsenian v.mohsenian@usc.ac.ir Department of Civil Engineering, University of Science and Culture, PO Box 13145-871, Park Avn., Ashrafi Esfahani Blv., Tehran, Iran

degree-of-freedom (SDOF) systems for building frame structures and considered maximum roof displacement and inter-storey drift demands. In another relevant study, Zhang et al. (2007) developed a damage index based on a linear combination of dissipated energy and structural deformation demands, with different weights assigned to each part.

Banon and Veneziano (1982) experimentally calibrated a damage index based on rotation and curvature ductility and dissipated hysteresis energy to predict the failure probability of concrete structures. Powell and Allahabadi (1988) proposed a method to determine the damage index based on plastic deformations. Through a comparative investigation of SDOF systems, Cosenza et al. (1993) showed that the damage indicators proposed by (Banon and Veneziano 1982; Park, Ang, and Wen 1987; Powell and Allahabadi 1988) could be linked with setting appropriate parameters in the damage models. In another study, Guan and Karbhari (2008) proposed a damage index based on modal displacements and rotations through experimental and numerical studies. They showed that the proposed damage model could resolve the deficiencies of modal curvature-based damage models.

Roufaiel and Meyer (1987) suggested "modified flexural damage ratio" and "global damage parameter" for component-level and system-level seismic damage assessment, respectively. The modified flexural damage ratio is based on the changes in the stiffness, moment and curvature of the member, whereas the Global Damage Parameter depends on the displacement responses of the entire structure.

Colombo and Negro (2005) proposed a damage index that applies to all construction materials based on structural resistance capacity degradation. Wang et al. (2007) offered an indicator to assess the safety of the storeys of a building based on modal shapes and frequencies and applied the indicator to Van Nuys Building in order to compare the results with visual inspection outcomes.

Falerio et al. (2008) proposed an energy-based damage model for the concrete structural members and provided the methodology to implement the model in finite element analysis. Rodriguez (2015) proposed a seismic damage index for SDOF systems by comparing the energy dissipated by an inelastic SDOF system with the energy absorbed by the same system with linear elastic response. The proposed damage index was then used to determine the damage level of different structural systems with different ductility capacities using their equivalent SDOF systems (Rodriguez 2018). He et al. (2022) proposed a damage model based on the differential ratio of elastic-plastic dissipated energy by determining the difference between the ideal elastic – plastic deformation energy and the actual elastic – plastic deformation energy. The damage state limits were calibrated based on the story drift ratio ranges, and the proposed model was experimentally verified for concrete structures under static and seismic loads.

Other implicit damage indicators are proposed besides commonly used EDPs (e.g. rotation, displacement, energy). In the Endurance Time method (Estekanchi, Arjomandi, and Vafai 2008), the target time within which the system remains stable under an intensifying acceleration function represents the damage index and the performance level at a specific earthquake intensity. Mohebi et al. (2019) proposed a new damage index for steel frames based on the spectral acceleration and the maximum inter-storey drift as general response and local damage parameters, respectively.

As nonlinear deformations are intrinsically linked to damage and other EDPs, such as ductility, it looks more appropriate to define the damage level in relation to deformation parameters. For instance, the relative displacement of adjacent storeys, or inter-storey drift, can be used as a basic and simple global damage indicator. So far, attempts have been made to connect damage state to either maximum drifts or residual drifts under an earthquake event. In some seismic codes, the maximum drift and residual drift parameters have been introduced as a criterion to assess the performance level in lateral force-resisting systems (ASCE 2007; HAZUS 1997). Despite the shortcomings associated with these simple indicators, they are widely used to estimate earthquake-induced damage to buildings.

Sozen (1981) described the damage state of structures as a ratio involving the maximum inter-storey drift. Ghobarah et al. (1999) showed that the drift values corresponding to different damage states are significantly affected by the element types and structural systems. By defining a drift range corresponding to different damage levels for structural systems with different ductility properties, they also found that the existing drift limits are conservative for ductile systems while not for non-ductile

systems (Ghobarah, Abou-Elfath, and Biddah 1999). Zaker Esteghamati et al. (2018) studied the effect of design drift limit on the seismic performance of reinforced concrete dual high-rise buildings. They showed that considering a larger design drift limit does not induce a significantly higher risk but results in a more cost-effective design.

Jalayer et al. (2007) introduced the concept of employing a scalar damage measure (DM) for conducting probabilistic seismic performance assessments and reliability analyses of reinforced concrete (RC) frames. The suggested index is defined as the demand-to-capacity ratio of critical structural components leading to structural failure and accommodates the uncertainty inherent in the input earthquake record. In a subsequent study, Jalayer et al. (2015) proposed the use of Cloud Analysis for fragility assessments of RC frames. This method relies on a large sample of Monte Carlo simulations and is capable of considering both record-to-record variability and uncertainties associated with structural modeling. However, these approaches require the computation of local performance parameters for all structural elements, a process that can be time-consuming, particularly for large structures with numerous structural elements.

Yang et al. (2010) investigated the inter-storey drifts of buildings under various near-fault ground motions, and Palermo et al. (2017) conducted extensive studies to evaluate and predict the maximum inter-storey drifts in frames equipped with viscous dampers excited by seismic loads.

By proposing the limit values of the maximum drift corresponding to different performance levels, Mohsenian and Mortezaei (2019) provided a damage function to estimate the damage level for two different height ranges of box-type reinforced concrete systems. Dai et al. (2017) assessed the seismic damage of a four-story reinforced concrete building through empirical equations of the residual drift results. They found that using residual drift values results in a high uncertainty degree in damage estimation. Mibang and Choudhury (2021) also presented a methodology to evaluate the global damage index for frame shear wall buildings using a combination of EDPs, including inter-storey drift ratio, joint rotation, and optimum roof displacement. They calibrated a linear function that was only compared with another global damage index (Park-Ang).

The critical study of the methods discussed above reveals that the majority of the proposed damage indices are directly derived from the dissipated energy in the structural system. While these indices are generally suitable for assessing the extent of damage, their practical application in structural analysis has been limited due to computational challenges and the requirement of specialized software and/or detailed non-linear models. To address this issue, drift-based damage index has been introduced in most seismic design codes. Although this index is well-known in the engineering community, its application in performance-based analysis and design still lacks clarity.

Despite its simplicity and widespread applicability of the maximum drift in damage estimation, the latest editions of some of the widely used seismic standards (e.g. ASCE 2017) have excluded this measure as a global damage index. Instead, the new seismic codes generally recommend using local damage indicators such as plastic rotations for the seismic performance assessment of various structural systems. While these methods can significantly enhance the accuracy and reliability of seismic analyses, they require multiple checks to assess the status of each structural (or non-structural) element to determine the overall damage level of the structure. This can limit the practical applications of the local damage assessment for performance-based analysis and design purposes, especially in the preliminary design phase.

The above discussions emphasize the importance of developing simple yet reliable functions to estimate local and global damage in the structural system by utilizing a practical response measure, such as maximum inter-story drift. To adopt the proposed method for the performance-based design and assessment of structures, it is also necessary to establish response limits corresponding to different performance levels (e.g. Immediate Occupancy (IO), Life Safety (LS), and Collapse Prevention (CP)) using a reliability-based approach. The present study aims to address these issues by focusing on multi-storey steel moment-resisting frames.

The first section covers the current literature in this area. In the second section, the problem statement is provided along with the proposed methodology. The third section elaborates on the

studied models, providing detailed explanations regarding the initial design of the selected frames and their nonlinear modeling. The fourth section describes the adopted approach for computations, wherein the frames are analyzed using incremental dynamic analysis and seismic reliability assessment. In this section, appropriate maximum inter-story drift values are estimated for different performance levels. The fifth section proposes a linear function, based on the previously determined limit values, which offers a straightforward means to estimate the system's damage by relying on the maximum inter-story drift response. The sixth section validates the established maximum limit values of inter-story drifts (obtained in Section 4), as well as the developed damage function (derived in Section 5), across various performance levels. The seventh section examines the level of confidence in the maximum inter-story drift limits presented in several widely used seismic codes. Finally, key findings of this study are presented in detail in the last section.

2. Methodology

Most conventional force-based seismic design codes (e.g. ASCE 2010; Eurocode 2005; Standard No. 2800 2014) introduce parameters such as behavior factor (R) and displacement amplification factor (C_d) permitting the utilization of linear models in the initial stages of structural design. This approach has streamlined the structural design process and eliminated the necessity of developing and analyzing nonlinear models.

In this approach, the structural stiffness is mainly controlled by satisfying the requirement of maximum inter-story drift limits. As shown in the schematic Fig. 1, the model is initially analyzed within the linear behavior range, and the vertical distribution of the maximum inter-story drift response ($Drift_0$) is then obtained. Since these results do not account for the effects of nonlinear behavior of members and are not realistic, they are multiplied by the displacement amplification factor (Cd). By knowing the actual vertical distribution of the maximum inter-story drift response ($Drift_m$) and comparing it with the allowable limit values ($Drift_a$), the adequacy of the design and the measure of stiffness in the system are evaluated. Utilizing a nonlinear model, the actual response of the maximum inter-story drift ($Drift_m$) is directly obtained from the structural analysis. In this case, comparing the results with the allowable values corresponding to different performance levels determines the structural performance level.

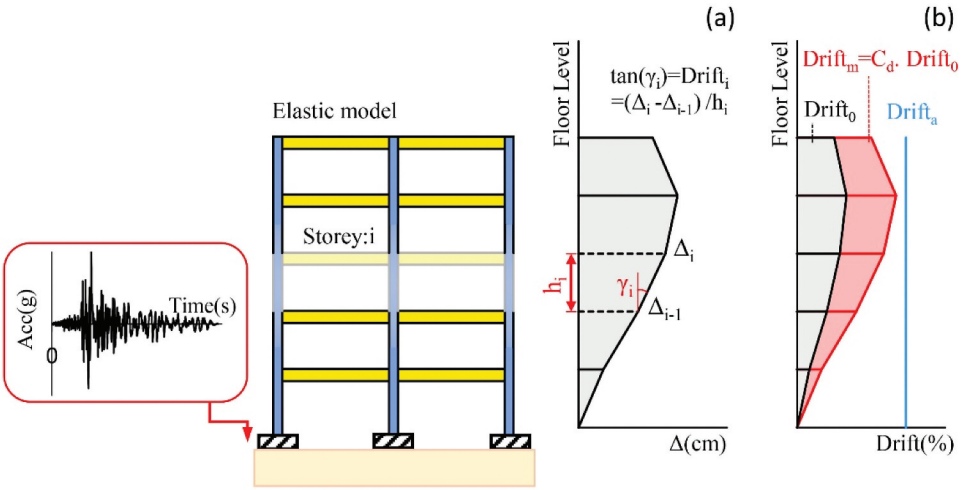

Figure 1. Linear analysis of a hypothetical frame: (a) Determining floor displacement responses and introduction of maximum inter-story drift parameter, and (b) Comparison between the actual inter-story drift response with allowable limit values.

C_d and $Drift_a$ are comprehensively described in the seismic design codes, where appropriate quantitative values are provided for each parameter. However, the efficacy and adequacy of these parameters, as well as the level of confidence in their limit values, remain uncertain. On the other hand, they are generally presented for a specific level of performance and earthquake intensity level, e.g. Life Safety (LS) under Design Basis Earthquake (DBE). Performing a linear analysis and comparing the actual maximum inter-story drift response with appropriate limit values presents a straightforward scenario that avoids the complexities associated with nonlinear modeling and the computational costs of capturing and controlling local member responses. This scenario is also highly practical for nonlinear analyses and relies on considering the maximum inter-story drift as a global damage indicator in the system and assigning desirable limit values for it.

In the present study, allowable inter-story drift limit values are extracted for different performance levels, including Immediate Occupancy (IO), Life Safety (LS), and Collapse Prevention (CP), in steel moment frame systems. It should be noted that the computation process is conducted within a framework of reliability and is based on local damage indicators of the members, specifically the rotation of plastic hinges in beams and columns. Figure 2 provides a schematic overview of the workflow. To account for inherent uncertainties associated with earthquakes and potential failure modes in the system, the frames are subjected to incremental dynamic analyses using a set of ground motion records. For each performance level and record, the maximum inter-story drift is determined when the local response (rotation of plastic hinges in elements) reaches a certain specified limit value (e.g. θ_0). Consequently, for each performance level, the number of obtained inter-story drift values is equal to the number of the utilized records. By knowing the probabilistic distribution of the drift response and considering rational safety factors (S.F), a desirable level of drift ($Drift_a$) is chosen for the system at each performance level.

With the establishment of allowable limit values for different performance levels (i.e. $Drift_a = Drift_{IO}$, $Drift_{LS}$, and $Drift_{CP}$), a function can be proposed for assessing the extent of damage (local and global) in the system, while the results can be also used to evaluate the adequacy of the existing limit values outlined in the seismic design codes. Furthermore, these values are essential for determining displacement amplification factors (C_d) and ensuring compliance with the corresponding coefficients specified in the codes.

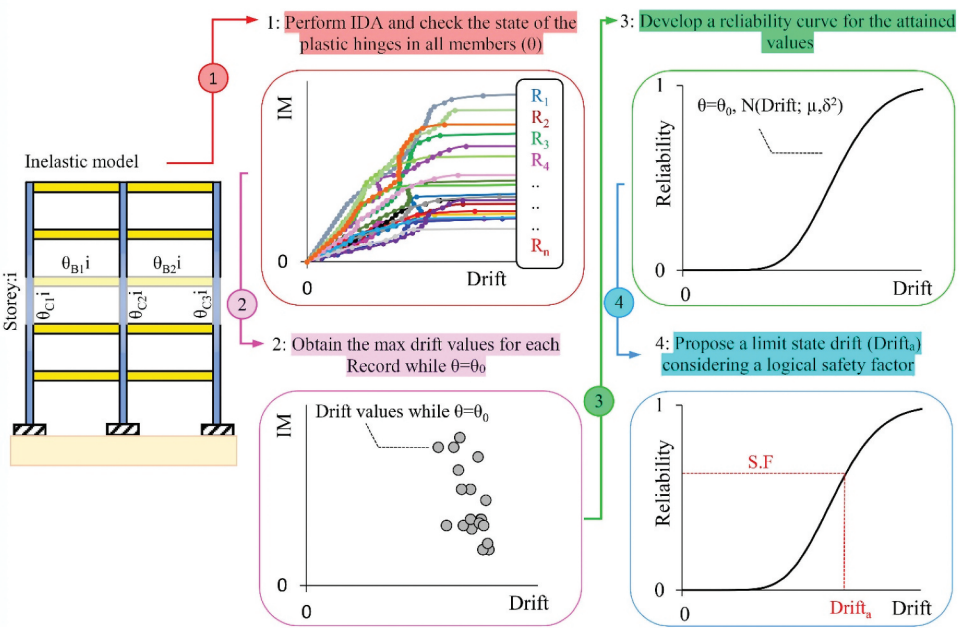

Figure 2. The procedure of obtaining limit values of inter-story drift for a global performance level corresponding to local response θ_0 in members.

3. Specifications of the Studied Models

To assess the efficiency of the proposed methodology, steel intermediate moment-resisting frames (medium ductility) have been considered in this study (see Fig. 3). All the frames have a similar horizontal plan, with a span length of 5 m and a storey height of 3.2 m. To account for the building height effects, three different buildings with a different number of floors (n) have been studied, where n is equal to 5, 10, and 15. The dead load (Q_D) and the live load (Q_L) with a magnitude of 31.5 kN/m and 10 kN/m have been applied to the floors respectively, except for the roof level where its live load is set as 7.5 kN/m. While using 2D models in general disregards the torsional effects on the displacement responses of structures, it was not considered to be a major limitation in the context of this study as the selected structures exhibit symmetry in both plan and elevation, reducing the potential effects of torsion.

The structures are assumed to be residential buildings located in a very high seismic-prone zone (Peak Ground Acceleration = 0.35 g; according to Iran's Standard No 2800 (2014)). The site soil is assumed to be type C (very dense soil and soft rock with a shear wave velocity between 360 m/s and 760 m/s) according to the standard classification by ASCE (2010). The studied frames have been designed according to the Institute of National Building Regulations (DCSS 2013) using the ETABS software (CSI 2015). Hollow Structural Sections (HSS) have been used for the columns, while I-shaped sections have been used for the beams. Since the selected structures are symmetric in plan, HSS columns are used as they exhibit symmetric behaviour about their local axes and can provide uniform flexural and shear capacities in both directions. However, previous studies demonstrated that W sections can also provide a viable solution for columns as they exhibit no more than a 10% deterioration in strength when subjected to axial loads below 75% of their nominal yield strength, even under significant inter-story drift ratios expected during a strong earthquake event (Newell and

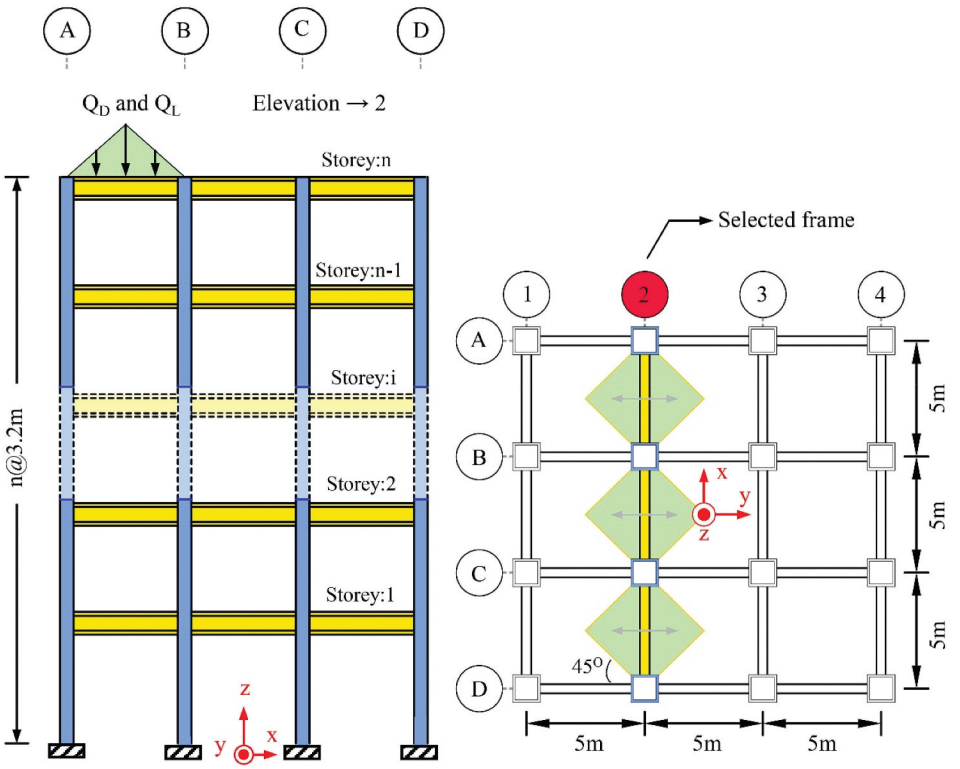

Figure 3. The geometry and loading conditions of the studied frames.

Uang 2008). The specifications of the cross-sections used for the beam and column elements are shown in Fig. 4 and are all listed in Table 1. The geometry, element sections, and loading conditions are symmetrical with respect to the vertical axis (z) for all the frames. The effect of rigid diaphragms has been considered at the floor levels.

The utilized material in the analysis is mild steel (A36) with a yield strength of 250 MPa, a Poisson's ratio of 0.26, and a Modulus of Elasticity of 200 GPa (ASTM 2019). The expected yield strength of steel materials (F_{ye}) has been considered to be 1.15 times the nominal yield strength (F_y) (ASCE 2017), such that $F_{ye} = 1.15\ F_y$ and $F_y = 250$ MPa.

The results of eigenvalue analyses on the studied frames are reported in Table 2, where the effective mass factors (M) and the vibration periods (T) for the first three vibrational modes are shown.

It should be noted that the proposed probabilistic assessment method is general and can be easily applied to other structural systems. While the frames used in this study are designed based on the regulations currently used in Iran, the selected design assumptions are not expected to influence the overall application of the proposed framework.

The PERFORM-3D software (CSI 2017) has been used for the nonlinear analysis of the frames, and the modeling details are described in the following.

The effects of gravity load Q_G in the linear and nonlinear ranges and for gravity and lateral load combination have been taken into account using the following equation (ASCE 2017):

$$Q_G = Q_D + 0.25Q_L \tag{1}$$

where Q_D and Q_L respectively denote the dead and live loads.

The generalized load-displacement relationship for beam and column elements has been adopted, as depicted in Fig. 5. Parameters a, b, and c in the plot have been set according to ASCE (2017), which

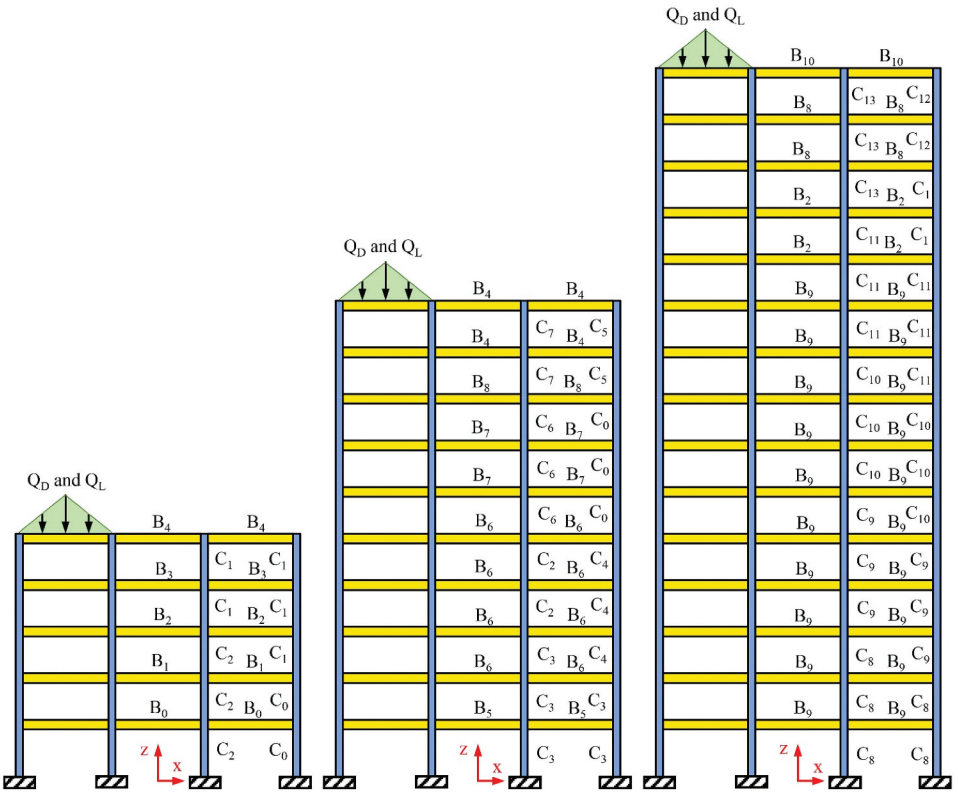

Figure 4. Details of the cross-sections used for structural elements of the studied frames.

Table 1. Specifications of the cross-sections used for beam and column elements (values in mm).

Columns		Beams	
ID	Section (width × thickness)	ID	Section (width × thickness)
C_0	HSS (350 × 15)	B_0	Web(350 × 10)-Flanges(180 × 20)
C_1	HSS (300 × 15)	B_1	Web(350 × 10)–Flanges(200 × 20)
C_2	HSS (400 × 20)	B_2	Web(300 × 10)–Flanges(200 × 20)
C_3	HSS (500 × 20)	B_3	Web(270 × 10)–Flanges(150 × 20)
C_4	HSS (400 × 15)	B_4	Web(240 × 10)–Flanges(150 × 20)
C_5	HSS (250 × 15)	B_5	Web(300 × 15)–Flanges(180 × 15)
C_6	HSS (300 × 20)	B_6	Web(350 × 10)–Flanges(250 × 25)
C_7	HSS (200 × 20)	B_7	Web(350 × 10)–Flanges(200 × 25)
C_8	HSS (650 × 25)	B_8	Web(270 × 10)–Flanges(180 × 20)
C_9	HSS (550 × 25)	B_9	Web(350 × 10)–Flanges(300 × 20)
C_{10}	HSS (450 × 20)	B_{10}	Web(200 × 10)–Flanges(150 × 20)
C_{11}	HSS (350 × 20)	–	–
C_{12}	HSS (240 × 15)	–	–
C_{13}	HSS (270 × 15)	–	–

Table 2. Effective mass and period of vibrations of the first three modes of the studied frames.

	5-storey		10-Storey		15-Storey	
Mode No.	*T*(sec)	*M*(%)	*T*(sec)	*M*(%)	*T*(sec)	*M*(%)
1	1.07	76.9	1.78	73.4	2.43	70.4
2	0.38	14.1	0.75	13.1	0.97	13.0
3	0.19	4.8	0.42	5.4	0.55	5.2

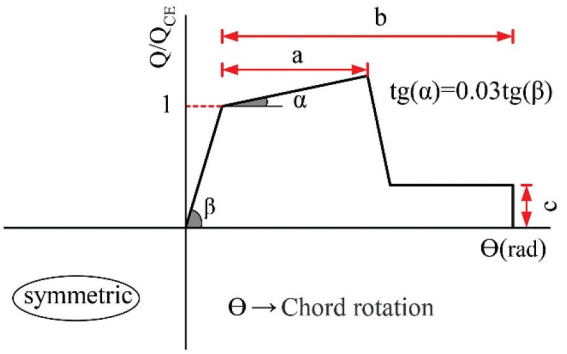

Figure 5. Generalized load-displacement response adopted for the steel members.

includes the modelling guidelines and acceptance criteria for the nonlinear analysis of steel components. Accordingly, the slope of the initial hardening stage of steel (*tg(α)*) is set to be 3% of the slope of the elastic branch (*tg(β)*) (ASCE 2017).

Q_{CE} represents the flexural strength of the compact members at yielding. For beam elements, it is given by:

$$Q_{CE} = ZF_{ye} \tag{2}$$

while for column elements, it is instead given by:

$$Q_{CE} = ZF_{ye}\left(1 - \frac{|P|}{2P_{ye}}\right) \text{if} \left(\frac{|P|}{P_{ye}} < 0.2\right) \tag{3}$$

$$Q_{CE} = \frac{9}{8}ZF_{ye}\left(1 - \frac{|P|}{P_{ye}}\right) \text{if} \left(\frac{|P|}{P_{ye}} \geq 0.2\right) \tag{4}$$

where Z is the plastic modulus of the cross-section of the element; F_{ye} denotes the expected yield strength of the material; P is the axial force in the member at the beginning of the dynamic analysis; P_{ye} is the axial yield capacity of the member, computed as $P_{ye} = A_g F_{ye}$, A_g being the gross area of the cross-section.

To carry out the analyses in PERFORM-3D (CSI 2017), linear behaviour has been considered along the length of the elements, with nonlinearity incorporated as concentrated "*moment-rotation* " hinges at the two ends of each member where plastic hinges are potentially formed. The design and detailing of connections and panel zones in moment frame structures are typically performed such that the seismic fuses exhibit desired performance by preventing premature failure modes in connection zones. For this purpose, the design forces in these elements are estimated either by assuming the formation of plastic hinges at the fuses or through analyzing the structure under an intensified earthquake (e.g. three times larger than the design earthquake as suggested by Standard No. 2800 (2014)). As a result, nonlinear behavior is not usually expected in these elements. Thus, in the present study, the effect of connections and panel zones has been disregarded in the nonlinear modeling of the moment frames. The beam-column connections and the connections of columns at the base level in the frame models are all considered to be rigid. For nonlinear dynamic analyses, 5% damping ratio is considered using the conventional Rayleigh damping model in this study. While this approach may result in unrealistic damping forces in inelastic structures and lead to an underestimation of peak displacement demands (Zareian and Medina 2010), it is widely accepted that accurate predictions can be achieved by incorporating the appropriate hysteretic load-displacement response of structural elements (Smyrou, Priestley, and Carr 2011).

4. Drift Limits Corresponding to Different Performance Levels

To account for the uncertainties related to future earthquake events, Incremental Dynamic Analysis (IDA) and fragility analysis have been adopted in this study (Ang and Tang 2007; Mohsenian et al. 2020; Vamvatsikos and Cornell 2002). First, IDA was performed on the frames using possible ground motion records as input. A set of 20 pairs of ground motion (GM) records have been selected from the PEER database (Web Site: https://ngawest2.berkeley.edu). All the selected records correspond to far-field ground motions of strong earthquakes with high local magnitudes (i.e. Ms > 6.6), recorded on soil type C of ASCE (2017) (soil shear wave velocity of 360 m/s ≤ Vs ≤760 m/s), and at low to moderate distances from the earthquake epicenter (less than 42 km). The horizontal component with higher spectral acceleration values in the range of the vibration frequencies of the selected frames has been selected as the main component of each GM for further analysis. The selected ground motions and some characteristics of their main components are listed in Table 3. A similar set of earthquake records have been used in previous studies (e.g. Mohsenian, Filizadeh, and Hajirasouliha 2023), and it is shown that their average response has a very good agreement with the selected target design spectrum provided by the Iran's Standard No. 2800 (2014).

Peak Ground Acceleration (PGA) has been adopted as the Intensity Measure (*IM)*, while maximum drift of the storeys has been used as the Demand Measure (*DM)* (Vamvatsikos and Cornell 2004). It should be noted that the results obtained by the proposed framework are independent of the employed intensity parameter, so any other relevant parameter instead of PGA can be used as *IM*. The output of

Table 3. Main components of the selected earthquake events used in the incremental dynamic analysis.

Record	Earthquake& Year	Station	R[a](km)	Component	M_w	PGA(g)
R_1	Cape Mendocino, 1992	Eureka – Myrtle & West	41.97	90	7.1	0.18
R_2	Cape Mendocino, 1992	Fortuna – Fortuna Blvd	19.95	0	7.1	0.12
R_3	Cape Mendocino, 1992	Loleta Fire Station	25.91	270	7.1	0.26
R_4	Chi-Chi_ Taiwan, 1999	TCU042	26.31	E	7.6	0.25
R_5	Chi-Chi_ Taiwan, 1999	TCU070	19.0	E	7.6	0.25
R_6	Chi-Chi_ Taiwan, 1999	TCU106	15.0	E	7.6	0.16
R_7	Chi-Chi_ Taiwan, 1999	CHY046	24.1	W	7.6	0.19
R_8	Chi-Chi_ Taiwan, 1999	CHY041	19.8	N	7.6	0.64
R_9	Chi-Chi_ Taiwan, 1999	CHY010	20.0	W	7.6	0.23
R_{10}	Chi-Chi_ Taiwan, 1999	CHY034	15.0	N	7.6	0.30
R_{11}	Chuetsu-oki_ Japan, 2007	Joetsu Ogataku	17.93	NS	6.8	0.32
R_{12}	Darfield_New Zealand, 2010	Heathcote Valley Primary School	24.5	E	7.0	0.63
R_{13}	Iwate_ Japan, 2008	Tamati Ono	28.9	NS	6.9	0.28
R_{14}	Iwate_ Japan, 2008	Yuzawa Town	25.56	NS	6.9	0.24
R_{15}	Landers, 1992	Barstow	34.86	90	7.4	0.13
R_{16}	Loma Prieta, 1989	Coyote Lake Dam–Southwest Abutment	20.34	285	6.9	0.48
R_{17}	Northridge, 1994	Hollywood – Willoughby Ave	23.07	180	6.7	0.25
R_{18}	Northridge, 1994	Lake Hughes #4B - Camp Mend	31.69	90	6.7	0.10
R_{19}	Northridge, 1994	Big Tujunga, Angeles Nat F	19.74	352	6.7	0.24
R_{20}	San Fernando, 1971	Pasadena – CIT Athenaeum	25.47	90	6.6	0.11

[a]Closest Distance to Fault Rupture.

the analysis is represented by a relationship between the structural responses and the intensity of the records; results regarding all the studied frames are shown in Fig. 6. In these plots and our entire analysis, the structural response is measured through the maximum inter-storey drift, defined as the ratio between the relative lateral displacement of the adjacent floors and the storey height. The specific limit states labeled in the figure are all explained in detail in the following.

The outcomes of IDA have been exploited to determine the drift limits corresponding to different performance levels (considering local damage criteria for beam and column elements). First, the cumulative distribution function of the maximum drift values associated with each performance level has been obtained for all the studied frames (Baker and Cornell 2005; Mohsenian et al. 2021; Mohsenian, Hajirasouliha, and Filizadeh 2023). Then, the values corresponding to μ-δ, μ, and μ+δ of the cumulative density function (*f*) have been determined via Rosenblueth's method (Nowak and Collins 2012), where μ and δ are respectively mean and standard deviation. Finally, these values have been averaged for the studied structural frames (see Fig. 7 and Table 4). The comprehensive and detailed description of this process is presented in Appendix A.

The range of the drift values bounded by μ-δ and μ+δ of the cumulative density function has been considered as the performance range. Such ranges of drift values are specified for each performance level and shown in Fig. 8(a). Within each performance range and based on the desired margin of safety, a limit value for the maximum inter-storey drift can be proposed as representative. The procedure to determine such limit values for each performance level is presented in detail in the following.

For the drift values smaller than those related to IO, the system is expected to be in the near-elastic range and the structural members are all fully serviceable. This range is thus equivalent to the Operational (OP) level, for which the system undergoes at most very light damage. The range between IO and LS can be termed Damage Control (DC). Within this range, the damage is expected to be limited such that the system may be serviceable again after some minor repairs. Any damage linked to either IO or DC performance level can be classified as Light Damage. The range between LS and CP can be termed Limited Safety (LiS); although some extent of damage can be identified in the system experiencing this range, it is supposed to cause minimal casualties. Both LS and LiS ranges can be categorized as Moderate Damage states. At the CP performance level, the system experiences extensive damage and casualties, which are indeed representative of Severe damage. The range beyond the CP

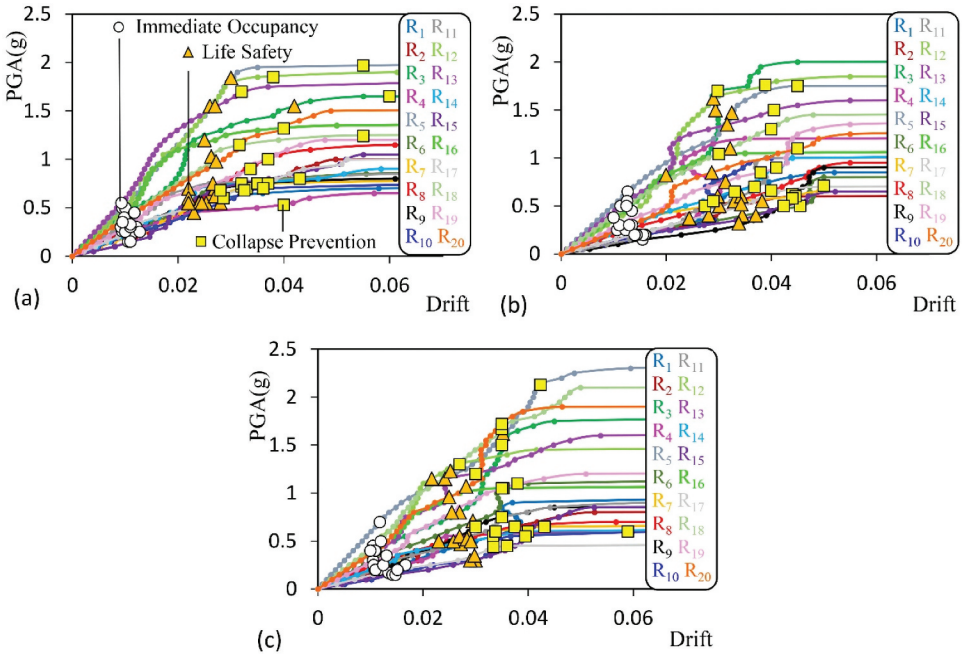

Figure 6. Results of the incremental dynamic analysis for the (a) 5- (b) 10- and (c) 15-storey frames, in terms of PGA vs drift for all the considered ground motion records. Symbols in the plots refer to the attainment of specified limit states.

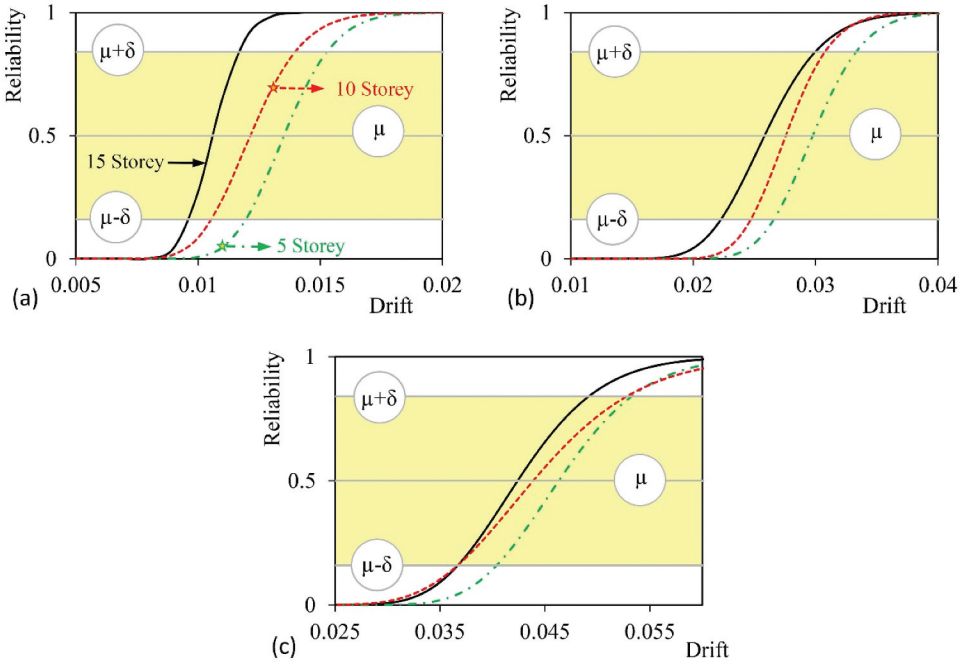

Figure 7. The cumulative distribution functions for the three studied frames: (a) Immediate occupancy, (b) Life safety, and (c) Collapse prevention performance levels, with the probability range between μ-δ and μ+δ highlighted.

Table 4. Drift values corresponding to μ-δ, μ and μ+δ, for each performance level (values are in %).

	Immediate Occupancy			Life Safety			Collapse Prevention		
Frame	μ-δ	μ	μ+δ	μ-δ	μ	μ+δ	μ-δ	μ	μ+δ
5-Storey	0.91	1.06	1.17	2.22	2.58	2.98	3.68	4.25	4.92
10-Storey	1.03	1.21	1.41	2.46	2.75	3.08	3.68	4.40	5.27
15-Storey	1.20	1.35	1.53	2.65	2.98	3.33	4.05	4.65	5.35
Average	1.05	1.21	1.37	2.44	2.77	3.13	3.80	4.43	5.18

can be linked to a complete collapse, and the system gets destroyed (D). It should be noted that other ranges around and in between those considered performance levels can represent other performance levels and damage states (see Fig. 8(b)).

In the present study, only IO, LS, and CP performance levels have been investigated. Referring to Fig. 9, in the proposed ranges every drift value corresponds to an exceedance probability value that can be derived from the fitted probability distribution function. For example, as shown in Fig. 9(a), when the rotation demand in the plastic hinges reaches the limit corresponding to IO performance level for the first time, regardless of the frame height, the maximum drift is almost surely greater than 0.5% and smaller than 2%. As mentioned earlier, for each range, a certain value of the drift can be selected as the limit state corresponding to a specific performance level; by selecting limit values close to the lower bound of the range, the structures will be associated with higher reliability.

The calculations of the probability distributions are thus entirely based on the values of local damage indices, by which the rotation in a plastic hinge reaches the values corresponding to a specific limit state. Therefore, limit values with a maximum probability of 50% in each range can be a target; this approach proves reliable, especially for structures of higher importance and for higher damage levels, with a dependence on the desired safety margin. However, for damage levels like IO, the limit values can be chosen from the values with higher probabilities, provided that the performance levels do not cross each other.

For the studied steel moment-resisting frames, the drift limit values corresponding to the IO, LS and CP performance levels are then proposed to be 1.2%, 2.5% and 4.5% (see Fig. 8(a)). According to Fig. 9(a), at the IO performance level, the probability of experiencing drift values smaller than 1.2% is 90% for 15-storey frame, 46.9% for 10-storey frame and 16.7% for the 5-storey frame. As shown in Fig. 9(b), at the LS performance level the probability of experiencing drift values smaller than 2.5% is instead 41.3% for the 15-storey frame, 18.7% for 10-storey frame and 11.6% for the 5-storey frame. Finally, at the CP

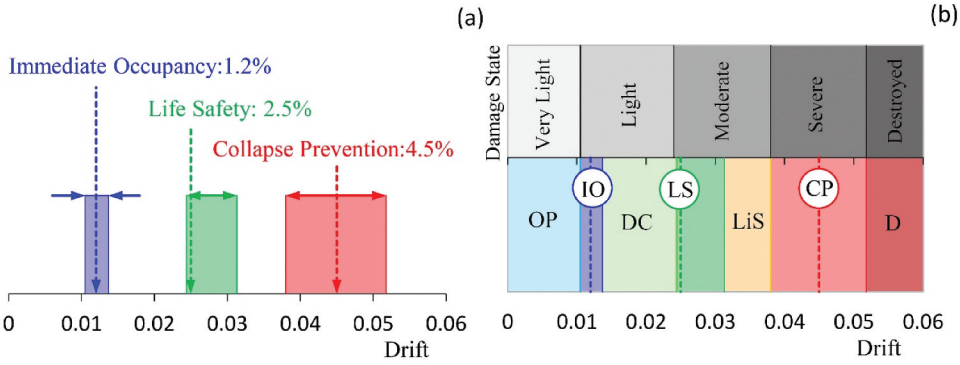

Figure 8. Inter-storey drift (a) Performance ranges and limit values determined for the three considered performance levels, and (b) Qualitative and quantitative descriptions of all the damage states and performance levels of the system.

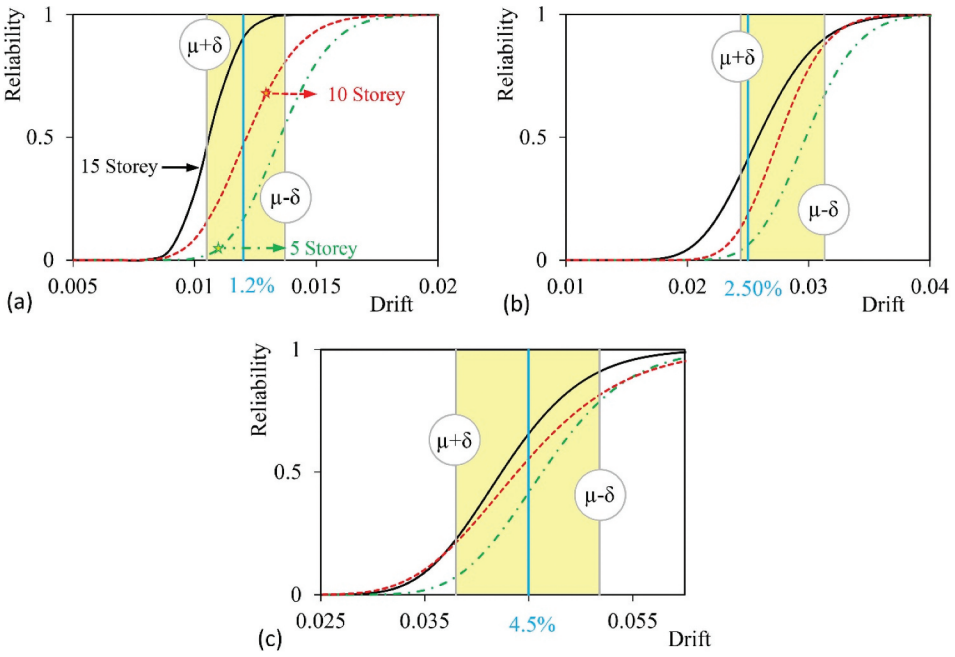

Figure 9. The cumulative distribution functions for the three studied frames, explicitly showing the performance ranges and the proposed limit values corresponding to (a) IO, (b) LS, and (c) CP levels.

performance level and according to Fig. 9(c), the probability of experiencing drift values smaller than 4.5% is 57.81% for the 15-storey frame, 50.5% for 10-storey frame and 35.5% for the 5-storey frame.

The proposed limit values are therefore expected to be able to estimate the corresponding performance levels of the system under different seismic intensities, with higher accuracy compared to the values proposed in seismic codes. This is investigated in the following section.

It should be noted that the above inter-storey drift limits are independent of the adopted analytical model and the analyses method, and do not require the assessment of local element responses. Therefore, for practical applications, simplified structural models in conjunction with any code suggested analyses method (e.g. push-over analyses) can be used as long as the maximum inter-storey drift can be estimated with a reasonable level of accuracy.

5. Proposed Damage Function

Grounding on the proposed limit values and the IDA results, a damage index based on the maximum inter-storey drift is here discussed and presented to estimate the performance level and the damage state of a steel moment-resisting frame subjected to earthquakes of different intensity levels. It is worth mentioning that "damage index" and "damage variable" are not interchangeable terms in the following discussion. A damage variable is assumed to display an initial value, dealt with as a kind of threshold and a critical value. If the damage variable is smaller or equal to the threshold value, the damage index DI is considered to be equal to 0, and the structure is assumed to be (practically) undamaged. If the damage variable attains its critical value instead, the index DI becomes equal to 1, and a structural failure is supposed to be approached. For all the values of the damage variable in between the threshold and the critical ones, a function can be defined to link the damage index and damage variable. In this range, the simplest relationship is the linear one adopted herein:

$$DI(D_m) = \frac{D_m - D_t}{D_u - D_t} \tag{5}$$

where D_m is the maximum inter-storey drift by into account the non-linear behavior of the structure; D_t is the damage threshold value; and D_u is the critical value of the maximum inter-storey drift. Depending on the definition of the critical damage level, D_u can take different values. In the present study it has been considered equal to 4.5%, which corresponds to the rotation in the plastic hinges leading to CP performance level in the structural members.

It can be noted that Eq. (5) is based on the concept of Demand to Capacity Ratio (DCR), which forms the foundation of conventional design processes and has been widely employed to assess the seismic performance of various structural systems (e.g. De Domenico and Hajirasouliha 2021; Jalayer, Franchin, and Pinto 2007). However, the damage function proposed in this study aims to establish a simplified relationship between the damage index and damage variables, utilizing an appropriate damage threshold, D_t. In this study, D_t is defined as the maximum inter-storey drift that corresponds to the onset of the nonlinear behaviour of the structure.

The inter-storey drift required for forming the first plastic hinge has been estimated to be around 0.5%, obtained by the dynamic analyses as explained in Section 4. By considering the lower bound limits on the ranges obtained for the IO and LS performance levels, several performance zones can be defined as follows (see Fig. 10):

- $D_m < D_t$ (DI = 0): The system behaves linearly (elastically), and no damage is developed.
- Zone 1 ($0 \leq$ DI < 0.15): Limited damage affects the system, but the performance level is still higher than the IO one. In this zone, rotations corresponding to the yield point are the upper limit that the members are expected to experience.
- Zone 2 ($0.15 \leq$ DI < 0.5): The yield point is exceeded in some beams, and the corresponding rotations in the plastic hinges attain the values corresponding to the IO performance level. In this zone, the structure has a performance level always higher than the LS one.
- Zone 3 ($0.5 \leq$ DI < 1.0): Several structural elements are affected by rotations beyond the IO performance level. The rotations in some elements reach the value corresponding to the LS performance level, but they are always smaller than the values required to attain the CP performance level.
- Zone 4 (DI > 1.0): The rotation in some plastic hinges reaches the value corresponding to the CP performance level.

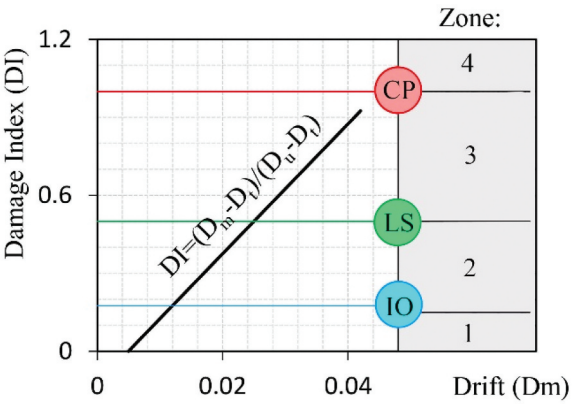

Figure 10. Proposed damage index for the steel moment-resisting frame systems.

As explained before, the proposed damage index model is independent of the adopted analytical model and the analyses method as it does not require the assessment of local element responses.

6. Validation of the Proposed Drift Limits and Damage Function

In order to validate the proposed inter-storey drift limit values and assess the accuracy of the damage function, 4-, 8- and 12-storey steel moment-resisting frames have been considered, as shown in Fig. 11. The height of each storey is 3.2 m, and the length of the spans is 5 m. The design process and the modeling assumptions for these frames, both in the linear and nonlinear ranges, are the same as described in Section 3. The specifications of the beam and column cross-sections are listed in Table 5. It should be noted that the validation frames are different compared to those used in the previous section.

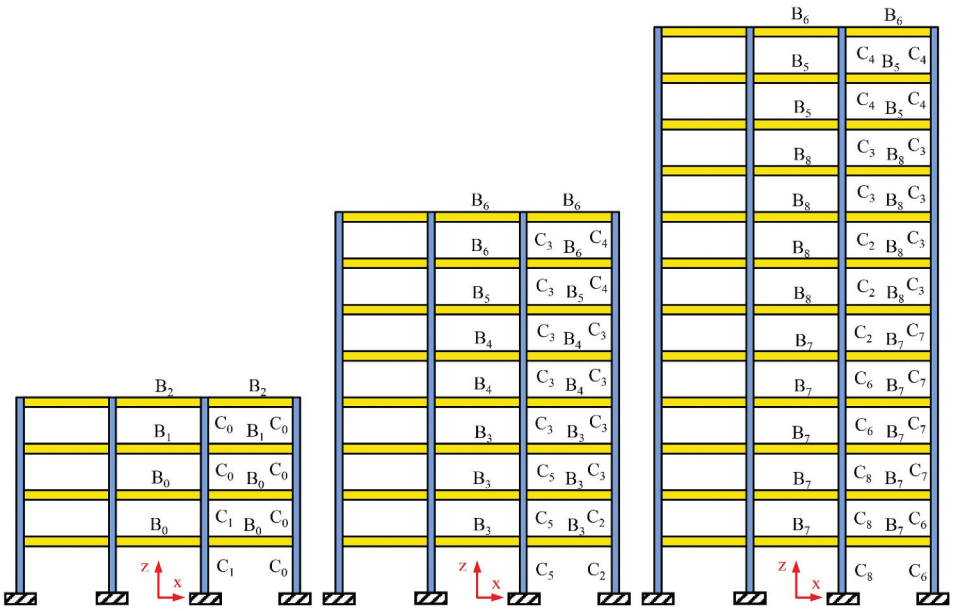

Figure 11. Selected frames for the validation process.

Table 5. Specifications of the cross-sections used for beam and column elements of the frames used in the validation process (values in mm).

Columns		Beams	
ID	Section (width × thickness)	ID	Section (width × thickness)
C_0	HSS (200 × 12)	B_0	Web(270×8)-Flanges(150×12)
C_1	HSS (240 × 12)	B_1	Web(240 × 8)-Flanges(150 × 12)
C_2	HSS (250 × 15)	B_2	Web(200 × 8)-Flanges(150 × 12)
C_3	HSS (200 × 15)	B_3	Web(300 × 8)-Flanges(150 × 15)
C_4	HSS (180 × 15)	B_4	Web(270 × 8)-Flanges(150 × 15)
C_5	HSS (270 × 15)	B_5	Web(240 × 8)-Flanges(150 × 15)
C_6	HSS (300 × 15)	B_6	Web(200 × 8)-Flanges(150 × 15)
C_7	HSS (240 × 15)	B_7	Web(300 × 8)-Flanges(180 × 15)
C_8	HSS (350 × 15)	B_8	Web(270 × 8)-Flanges(180 × 15)

The frames have been excited by an artificial ground motion record, shown in Fig. 12, which has been purposely scaled to different PGA values in order to represent different intensity levels. This record has been generated by modifying the existing earthquake ground motions using wavelet transforms (Hancock et al. 2006). Since the PGA of the main artificial record corresponds to the selected design level acceleration (= 0.35 g) and its response spectrum compares very well with the selected site-specific spectrum (Standard No. 2800 2014), it has been considered as the Design Basis Earthquake (DBE) in this study. Four different values of the factor have been then used to scale the record: 0.5, 1.0, 1.5, and 2.0. It should be noted that the present validation process can be carried out by using any arbitrary ground motion record with any intensity measure. Since an incremental dynamic analysis has been adopted to define the limit drifts and the damage function, the results are expected to be independent of the selected record and its intensity.

Via the nonlinear analysis of these frames, the maximum inter-storey drifts of the structures have been determined under the different earthquake intensity levels; their values are reported in Fig. 13.

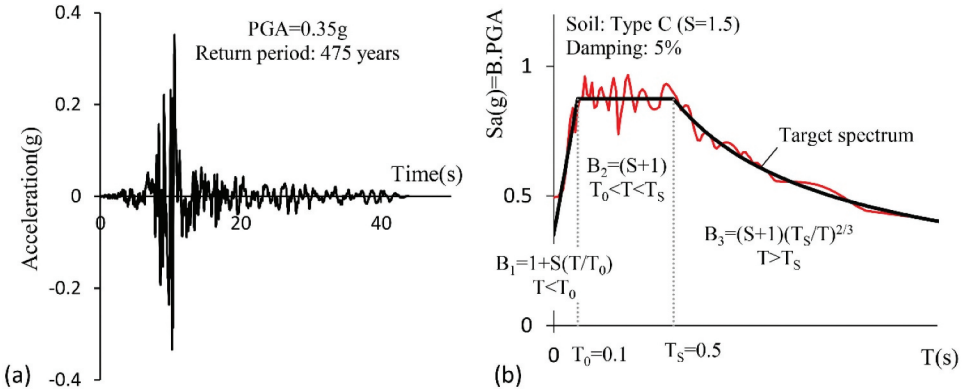

Figure 12. The generated artificial ground motion record: (a) Time-Acceleration; and (b) Comparison of the records response spectrum with the site-specific spectrum.

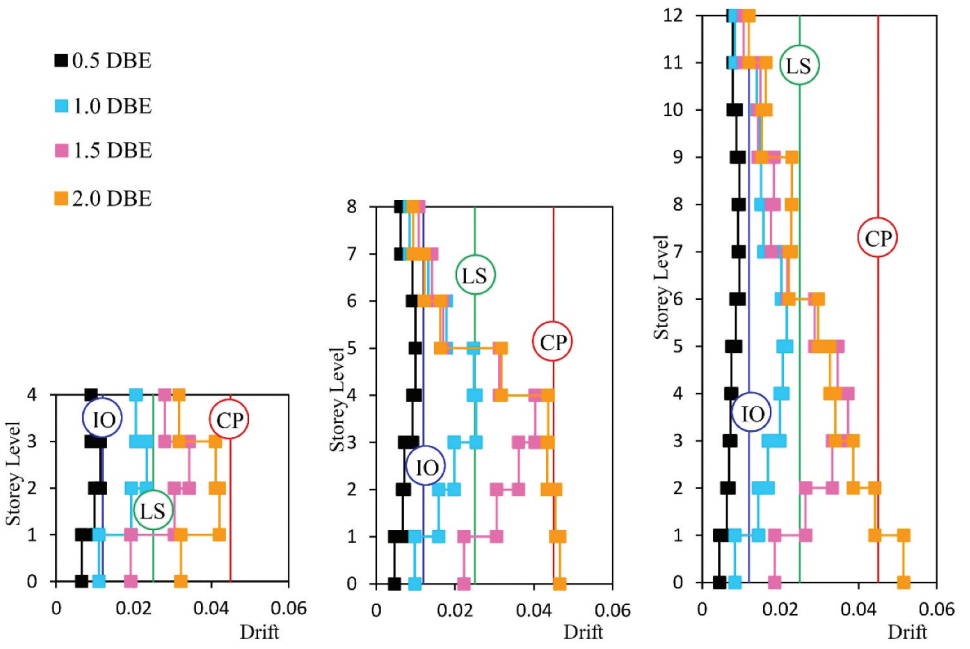

Figure 13. Distribution of the maximum drifts along the height of the frames, and the proposed drift limits for different performance levels.

Once the maximum drift demands are known, the damage index can be obtained from the damage function, as discussed in Section 5. The damage index has been computed for all the storeys of the considered frames, and the results are shown in Fig. 14. Given that the inter-storey drift is a global measure of the response, and our proposed damage index has been computed based on the drift demand, its maximum value among all the storeys is next adopted for further assessments.

By comparing the drift demands with the proposed limit states, the performance level of the frames under each earthquake intensity can be determined. As shown in Fig. 13, all the frames have a performance level higher than IO under a frequent earthquake with a PGA of 0.17 g (0.5DBE). Under the same earthquake intensity, the maximum value of the damage index in each frame is smaller than 0.15, being respectively equal to 0.14, 0.12, and 0.11 for the 4-, 8-, and 12-storey frames. It is therefore expected that, for this earthquake intensity, the plastic hinge rotation demands of all the structural elements are smaller than those corresponding to the IO level. As depicted in Fig. 15, the distribution of the plastic hinges and their state for all the frame elements under this intensity complies with the predicted drift limits and the damage indices.

The investigation of the maximum drift of the frames under the DBE with a PGA = 0.35 g has shown that all the drift values satisfy the LS performance level criterion. The relevant maximum damage index has proven to be smaller than 0.5, being equal to 0.45, 0.5, and 0.41 for 4-, 8- and 12-storey frames. For this earthquake intensity, the maximum rotations of the plastic hinges remain below the values corresponding to the LS level. As shown in Fig. 16, for this pattern of the plastic hinges the maximum rotation demand corresponds to rotations related to the IO level. The accuracy of the estimated drift limits and damage indices can be considered good also in this case.

By increasing the earthquake level to 1.5DBE, representing Maximum Credible Earthquake (MCE) with a PGA = 0.55 g, the performance level of the frames exceeds the threshold of the CP level (see Fig. 13). According to Fig. 14, the maximum damage index of the frames under this intensity level grows up to 0.73, 0.78, and 0.81 for 4-, 8-, and 12-storey frames. The maximum demands of plastic hinge rotation now exceed the LS performance level; this confirms the predicted state using the proposed drift values and damage function, as shown in Fig. 17.

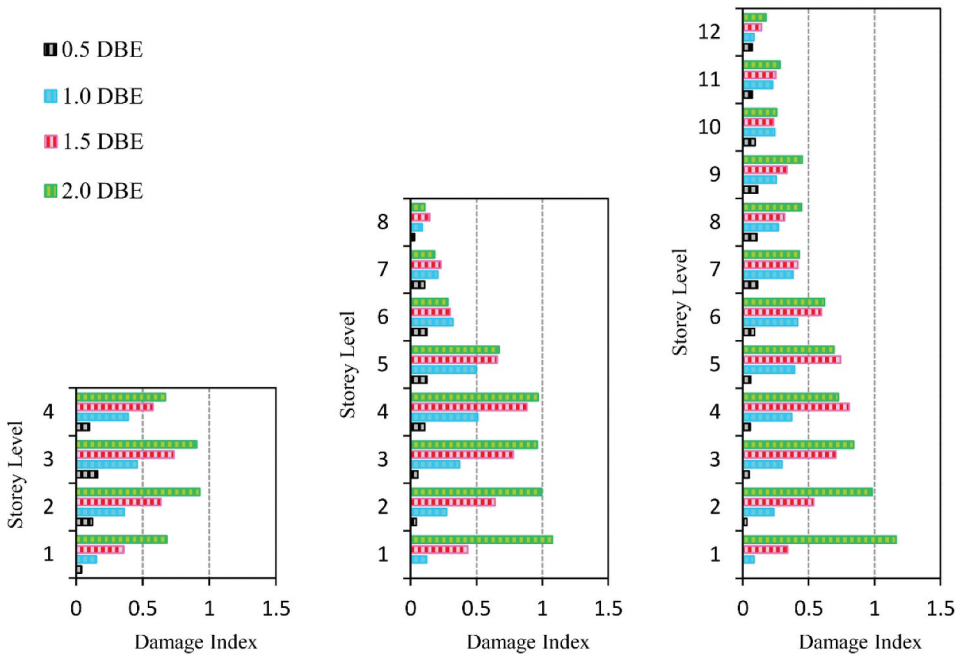

Figure 14. Damage indices computed on the basis of the maximum drifts of the frames under each seismic intensity level.

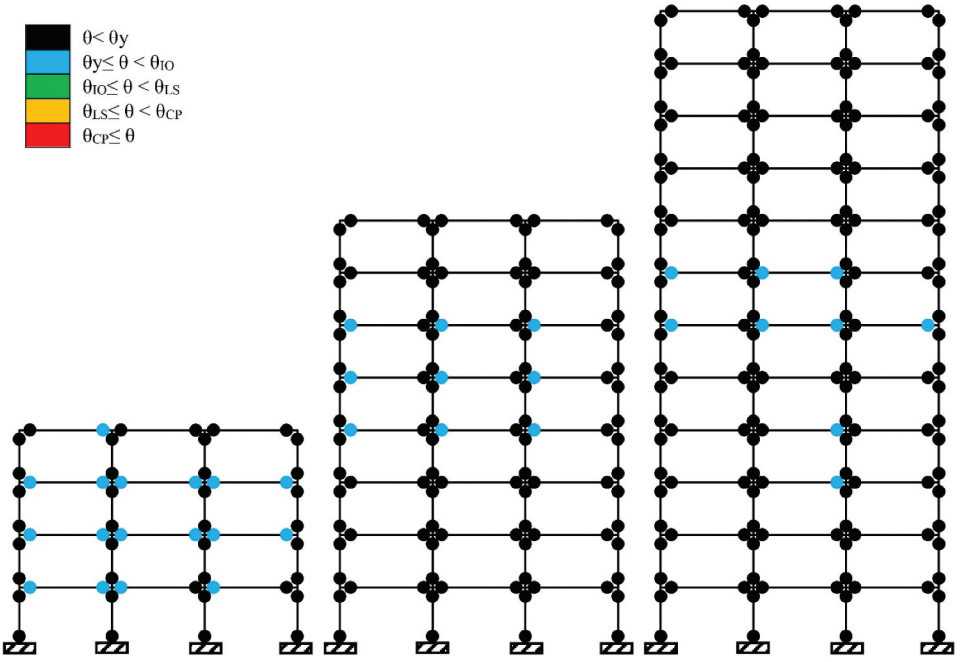

Figure 15. Distribution of plastic hinges, and relevant performance levels based on the local damage index under the frequent earthquake corresponding to 0.5DBE.

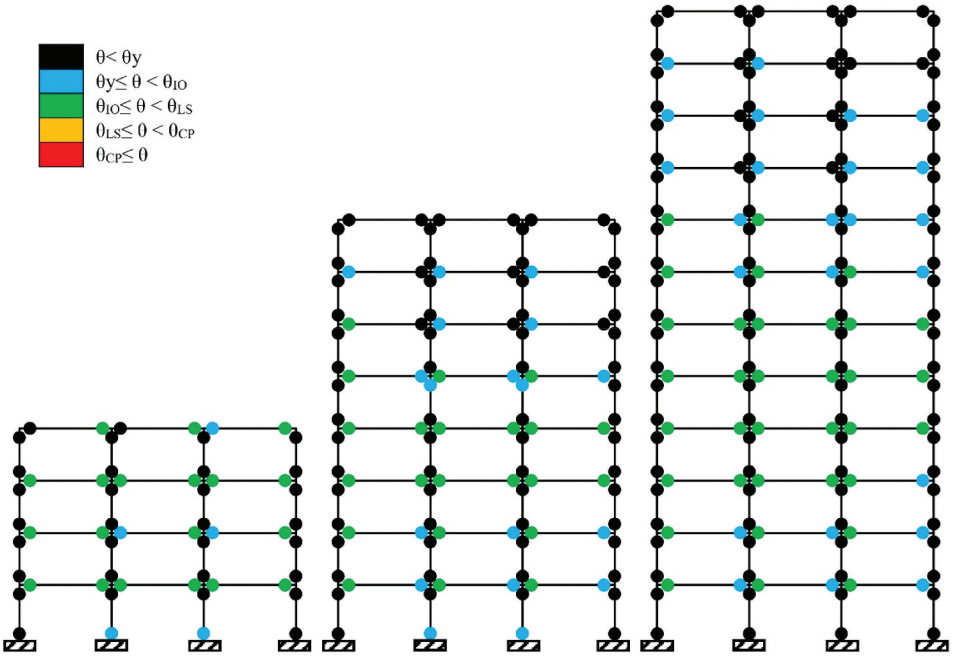

Figure 16. Distribution of plastic hinges, and relevant performance levels based on the local damage index under the design earthquake corresponding to 1.0DBE.

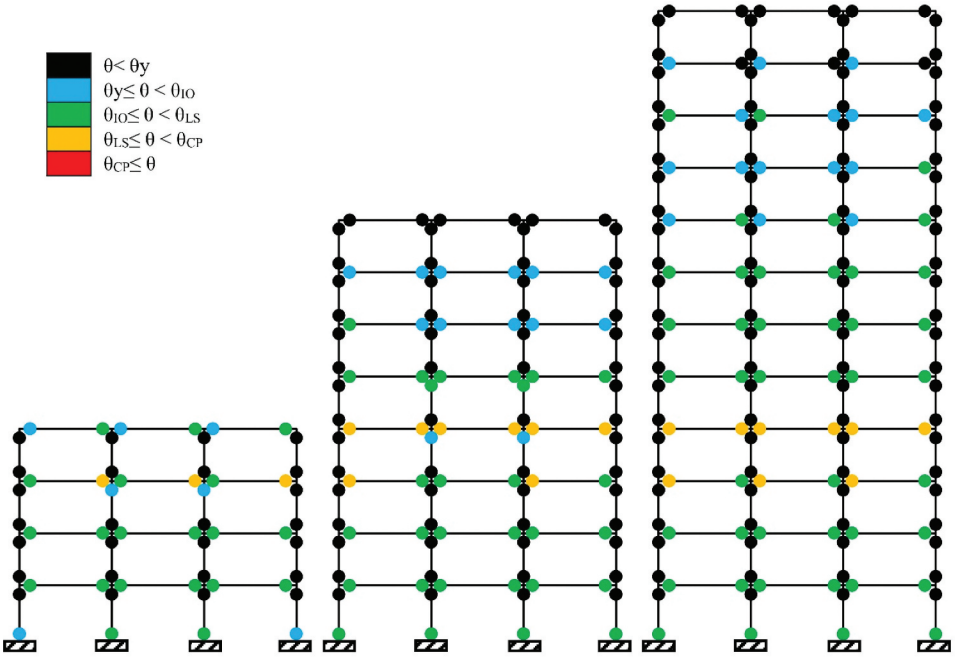

Figure 17. Distribution of plastic hinges, and relevant performance levels based on the local damage index under the MCE earthquake corresponding to 1.5DBE.

By further increasing the earthquake intensity to 2.0DBE, with a PGA = 0.70 g, the maximum inter-storey drift of the 4-story frame has resulted below the CP performance level, with a maximum damage index equal to 0.92. In this case, the maximum demands of plastic hinge rotation are expected to be smaller than the limit corresponding to the CP performance level. According to the drift criterion, the other two frames have instead attained the CP performance level, and their damage index is estimated as 1.1 for the 8-storey frame, and 1.2 for the 12-storey frame. For the two latter frames, it is thus expected that some structural elements experience rotations in the plastic hinges corresponding to the CP level. The predicted drift values and the proposed damage function are confirmed by the distribution of plastic hinges in the frames, as reported in Fig. 18.

In addition to estimating the situation of each plastic hinge in the system, the proposed damage function can predict the location of damage along the height of the frames with high accuracy. Hence, not only is the proposed damage function able to define the global damage, but it can also be used to estimate the intermediate (substructure) damage levels. This can be ascertained by comparing Figs. (15-18) with Fig. 14.

7. Comparison of the Proposed Limit Values with the Values Recommended in Seismic Codes

In this section, the proposed ranges and drift limit values for each performance level are compared with the performance limit values and damage states suggested by well-known and commonly used standards, such as ASCE (2007), ATC (1985), HAZUS (1997) and Eurocode 8 ([2005], 2022).

It should be noted that while some of the above-mentioned design guidelines may be outdated, they are still widely used by researchers and structural engineers due to their simplicity. On the other hand, these design guidelines provide inter-storey drift limits corresponding to different performance targets, and therefore, can be used to assess the limits proposed in this study.

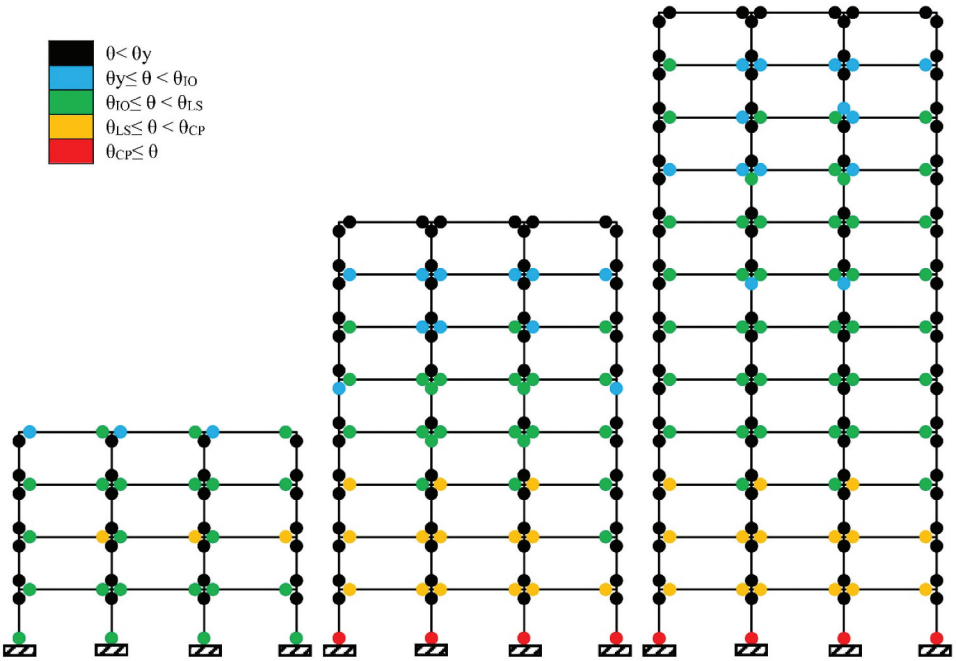

Figure 18. Distribution of plastic hinges, and relevant performance levels based on the local damage index under an earthquake corresponding to 2.0DBE.

7.1. ASCE41-06 standard

In ASCE (2007), the maximum drift limits suggested for steel moment-resisting frames at the IO, LS, and CP performance levels are 0.7%, 2.5% and 5%, respectively. As reported in Fig. 19(a), the ranges for LS and CP proposed in this study comply with the limits recommended by this standard. Regarding the CP level, the recommended drift limit is out of range and does prove conservative. Figure 9(a) also shows that, when the first rotation corresponding to the IO performance level is experienced, the maximum drift is certainly larger than 0.7%, regardless of the frame height. However, there seems to be an acceptable agreement between the limit values proposed in this study and those recommended by ASCE (2007).

7.2. ATC-13

In ATC (1985), regardless of the frame height, specific inter-storey drift ranges are proposed for different damage states; these ranges are all gathered in Table 6. According to Fig. 19(b), when the ranges recommended by ATC (1985) (top side of the chart) are compared with the performance ranges obtained in the present study (bottom side), it turns out that the IO performance range is a subset of the Moderate damage state. Since the reduction of the stiffness and resistance of the system are insignificant for the IO performance level, and the structure is expected to be serviceable after an earthquake event, it looks like the damage state consistent with this performance level is the Light damage one.

LS and CP performance ranges are both subsets of the Major damage state. At the LS performance level, the structure undergoes some damage, but its severity is not enough to cause casualties; on the contrary, at the CP performance level the structure experiences extensive damage, resulting in some casualties. Considering the system performance expectations at the mentioned levels, locating these two performance levels in one damage state range does not seem reasonable. Thus, the descriptions

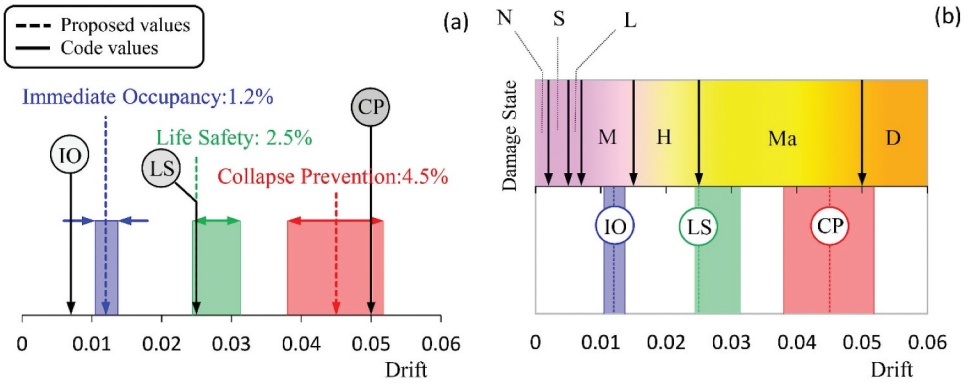

Figure 19. Proposed drift ranges for different performance levels, and comparison of the limit values with the values recommended in (a) ASCE41–06, (b) ATC-13.

Table 6. Drift values corresponding to different damage states in the system, according to ATC (1985).

Performance Level	Damage State	Inter-storey Drift, Δ (%)
1	None (N)	$\Delta < 0.2$
2	Slight (S)	$0.2 < \Delta < 0.5$
3	Light (L)	$0.5 < \Delta < 0.7$
4	Moderate (M)	$0.7 < \Delta < 1.5$
5	Heavy (H)	$1.5 < \Delta < 2.5$
6	Major (Ma)	$2.5 < \Delta < 5.0$
7	Destroyed (D)	$5.0 < \Delta$

and the ranges for system damage provided in ATC (1985) are not considered appropriate; using them for structural performance assessment under different intensity levels is accordingly not recommended.

7.3. HAZUS

In HAZUS (1997), specific limit states are provided for different damage levels, depending on the structure height, seismic design level, and the quality of construction. In this standard, frames with up to 3 floors are considered low-rise, frames with 4 to 7 floors are considered mid-rise, and frames with greater than eight floors are considered high-rise.

Table 7 shows the drift values corresponding to the damage states defined for low-rise frames with medium ductility. According to the recommendations in HAZUS (1997), the limit values for mid- and high-rise frames can be computed by multiplying the values for the low-rise frames by 2/3 and 1/2, respectively. In Fig. 20(a,b) the drift limit values recommended by HAZUS (1997) are compared with the ranges and values proposed in this study for different performance levels. According to the current study results, the drift limits and damage states proposed in HAZUS (1997) look misleading in some cases and cannot provide useful information related to the performance of the steel-moment resisting frames. Therefore, the use of the limit values suggested in HAZUS (1997) is not recommended for the seismic performance assessment of structures.

It should be noted that the presented results are limited to the adopted models and assumptions. While this study has specifically focused on the impact of varying the height of the frames, irregularities (in plan and height) and changes in frequency content and the properties of earthquake records can be also influential factors in the structural response. By employing a probabilistic approach and providing results in the form of performance intervals, it is expected that even with variations in model

Table 7. Drift values corresponding to different damage states in systems with medium ductility, according to HAZUS (1997).

Performance Level	Damage State	Inter-storey Drift (%)
1	Slight(S)	0.6
2	Moderate(M)	1
3	Extensive(E)	2.4
4	Complete(C)	6

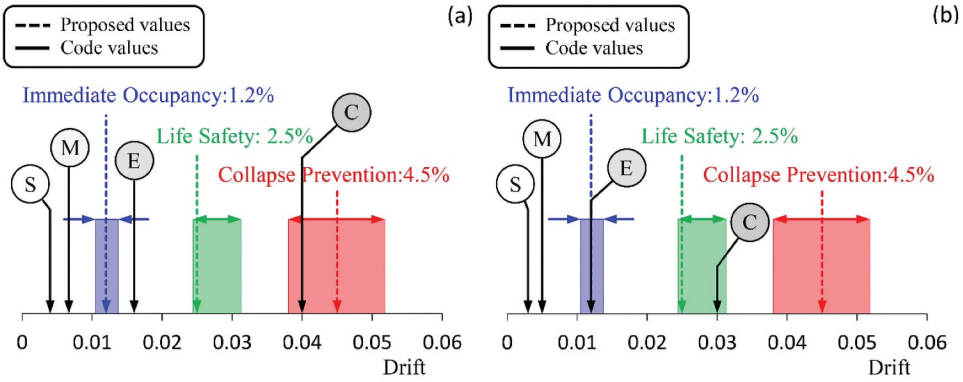

Figure 20. Proposed drift ranges for different performance levels, and comparison of the limit values with the values recommended in HAZUS: (a) 4-Storey frame, and (b) 8- and 12- storey frames.

characteristics and input excitations, the proposed intervals still encompass desirable values for the global damage index. Nevertheless, evaluating the sensitivity of the results to irregularities, as well as directionality pulses and near-fault effects, can provide a suitable basis for future studies.

In this study "maximum inter-story drift" during seismic loading has been investigated as a global damage index. This indicator has proven to be effective for evaluating the structural performance under an earthquake event during the analysis/design phase of the structure. However, for post-earthquake evaluations, the residual drift values should also be controlled. Providing corresponding quantitative values for the damage index of "residual drift" at different performance levels can serve as another area for further investigations.

The proposed damage function is established and calibrated based on the maximum inter-story drift experienced by structures during earthquake events. However, such functions can be adjusted for excitations other than earthquakes (e.g. noise and impact loads) and by considering parameters other than the maximum drift (such as frequency or dissipated energy). This provides an opportune avenue for further research. The adopted approach in this study is valid for various lateral load-resisting systems. Although the local responses may vary depending on the type of lateral load-resisting elements in the system, the process remains the same. Nevertheless, conducting a similar investigation for other commonly used lateral load-resisting systems can also provide a suitable basis for future research.

7.4. EUROCODE 8

In general, Eurocode 8 is a force-based design code that establishes inter-storey drift limits to control different limit states, including damage limitation (DL), significant damage (SD) and near collapse (NC). In the current version of the Eurocode 8 (2005), the maximum inter-storey drift limit depends on the type of non-structural elements and their interference with other structural elements, aiming to

satisfy DL under earthquakes with a 20% probability of exceedance in 50 years. The design inter-storey drift corresponding to SD limit state (d_r) can be calculated as follows (Eurocode 8 2005):

$$d_r = d_{r,DL}/v \tag{6}$$

where $d_{r,DL}$represents the design inter-storey drift ratio corresponding to DL limit state, which is equal to 1% if non-structural elements are fixed in a way that does not impede structural deformations. The reduction factor v is introduced to consider the variability in the return period associated with the damage limit requirement, with a recommended value of 0.5 for structures classified under importance classes I and II. In this scenario, d_r is calculated to be 2%. In the new version of the Eurocode 8 (2021), the drift limit to satisfy the Significant Damage (SD) limit state under the design seismic loads is also 2%, aligning with the provisions of the current version of the code (Tartaglia, D'Aniello, and Landolfo 2022).

Through a probabilistic approach, Gutiérrez-Urzúa et al. (2021) compared the capacity limits proposed by Eurocode 8 (2005) with those of ASCE (2007). They highlighted significant drawbacks in Eurocode 8 (2005) when estimating engineering demand parameters for steel moment-resisting frames. Figure 21 compares the drift ranges obtained in this study with the limit values suggested by Eurocode 8 (2005, 2021) corresponding to the Significant Damage (SD) limit state. It can be seen that the maximum inter-storey drift limit proposed by Eurocode falls within the values for Immediate Occupancy (IO) and Life Safety (LS) performance levels recommended in this study. This implies that the maximum inter-storey drift limit proposed by Eurocode 8 is conservative and is expected to meet the LS performance level criteria under the design earthquake.

8. Discussion and Conclusion

In the present study, a low computational cost reliability-based approach is proposed to assess the seismic performance range of steel moment-resisting frames based on maximum inter-storey drift ratios. While the proposed damage index can take into account the local damage indices defined at the structural element level, it does not require complex analytical models and/or computationally expensive analyses techniques. To set appropriate performance ranges, different drift limits were proposed as global performance indicators corresponding to Immediate Occupancy (IO), Life Safety (LS), and Collapse Prevention (CP) performance levels, by providing a link between maximum plastic

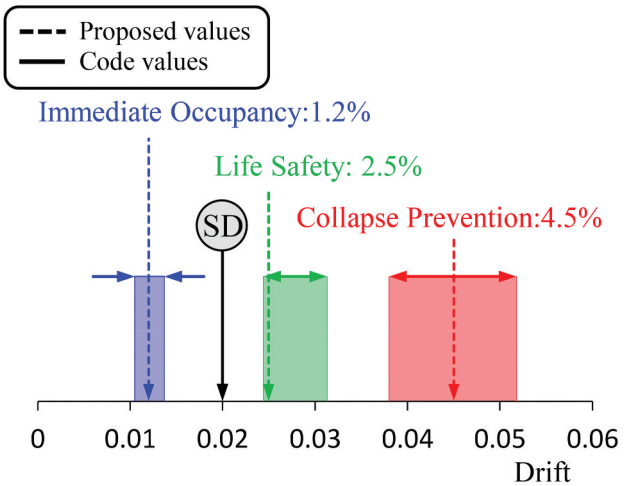

Figure 21. Proposed drift ranges for different performance levels compared to the limit value recommended by Eurocode 8 (2005, 2021) corresponding to significant damage (SD) limit state.

hinge rotations at critical members and maximum inter-storey drifts. It was shown that the proposed damage index could accurately evaluate the overall damage exhibited by a set of steel moment-resisting frames with different number of storeys subjected to a group of earthquakes of varying intensities. Subsequently, the proposed limit drift values corresponding to different performance levels were compared with those recommended in existing seismic codes. The main outcomes of the current study can be listed as follows:

(1) It is shown that the regulations in the existing design codes properly ensure the safety of structures under the design hazard level, and the moment-resisting frames accordingly designed satisfy the LS performance level under the design basis earthquake (475-year return period).
(2) By considering the plastic hinge rotation as a local damage indicator for structural elements subjected to earthquake, when one hinge first experiences a rotation corresponding to IO, LS and CP performance levels, the inter-storey drift limits handled as global damage index are respectively 1.2%, 2.5% and 4.5% for steel moment-resisting frames.
(3) The proposed damage function based on maximum inter-storey drift was shown to provide rather accurate estimates of the damage level in the whole structural system, despite its simplicity. The results also revealed the capability of the proposed damage function to estimate the location of damage in the buildings.
(4) The proposed performance ranges and the limit values obtained in this study are significantly different from the damage states and the corresponding limit values recommended in ATC-13 and HAZUS. The use of the values suggested in those standards could be misleading and lead to unsafe design solutions.
(5) The proposed performance ranges cover the limit values recommended in ASCE41-06 corresponding to the LS and CP performance levels. However, the ASCE41-06 limits recommended for the IO performance level are shown to be conservative.
(6) The maximum inter-storey drift limit proposed by Eurocode 8 (2005, 2021) corresponding to the Significant Damage (SD) limit state seems to be conservative and is expected to satisfy the LS performance level in steel moment-resisting frames.

Disclosure Statement

No potential conflict of interest was reported by the author(s).

ORCID

Vahid Mohsenian http://orcid.org/0000-0002-5918-1569
Reza Filizadeh http://orcid.org/0000-0002-9580-5121
Stefano Mariani http://orcid.org/0000-0001-5111-9800
Iman Hajirasouliha http://orcid.org/0000-0003-2597-8200

Data Availability Statement

The data that support the findings of this study are available from the corresponding author, upon reasonable request.

References

Ang, A. H.-S., and W. H. Tang. 2007. *Probability Concepts in Engineering: Emphasis on Applications to Civil and Environmental Engineering*. 2nd ed. Vol. 1. The University of Michigan; Wiley.
ASCE. 2007. *Seismic Evaluation and Retrofit of Existing Buildings, ASCE/SEI Standard 41-06*. Reston, VA: American Society of Civil Engineers.
ASCE. 2010. *Minimum Design Loads and Associated Criteria for Buildings and Other Structures, ASCE/SEI 7-10*. Reston, VA: American Society of Civil Engineers.

ASCE. 2017. *Seismic Evaluation and Retrofit of Existing Buildings, ASCE/SEI Standard 41-17*. Reston, VA: American Society of Civil Engineers.
ASTM. 2019. *ASTM A36/A36M-19, Standard Specification for Carbon Structural Steel*. West Conshohocken: ASTM International.
ATC. 1985. *Earthquake Damage Evaluation Data for California, ATC-13*. Redwood City, CA: Applied Technology Council.
Baker, J. W., and C. A. Cornell. 2005. "A Vector Valued Ground Motion Intensity Measure Consisting of Spectral Acceleration and Epsilon." *Earthquake Engineering and Structural Dynamics* 34 (10): 1193–1217. https://doi.org/10.1002/eqe.474.
Banon, H., and D. Veneziano. 1982. "Seismic Safety of Reinforced Concrete Members and Structures." *Earthquake Engineering and Structural Dynamics* 10 (2): 179–193. https://doi.org/10.1002/eqe.4290100202.
Colombo, A., and P. Negro. 2005. "A Damage Index of Generalised Applicability." *Engineering Structures* 27 (8): 1164–1174. https://doi.org/10.1016/j.engstruct.2005.02.014.
Cosenza, E., G. Manfredi, and R. Ramasco. 1993. "The Use of Damage Functionals in Earthquake Engineering: A Comparison Between Different Methods." *Earthquake Engineering and Structural Dynamics* 22 (10): 855–868. https://doi.org/10.1002/eqe.4290221003.
CSI (Computers and Structures Inc.). 2015. *Structural and Earthquake Engineering Software, ETABS, Extended Three Dimensional Analysis of Building Systems Nonlinear, Version 15.2.2*. Berkeley, CA.
CSI (Computers and Structures Inc). 2017. *Structural and Earthquake Engineering Software, PERFORM-3D Nonlinear Analysis and Performance Assessment for 3D Structures, Version 7.0.0*. Berkeley, CA.
Dai, K., J. Wang, B. Li, and H. P. Hong. 2017. "Use of Residual Drift for Post-Earthquake Damage Assessment of RC Buildings." *Engineering Structures* 147 (2017): 242–255. https://doi.org/10.1016/j.engstruct.2017.06.001.
DCSS. 2013. *Design and Construction of Steel Structures, Institute of National Building Regulations, Topic.10*. Iran: Ministry of Roads and Urban Development.
De Domenico, D., and I. Hajirasouliha. 2021. "Multi-Level Performance-Based Design Optimisation of Steel Frames with Nonlinear Viscous Dampers." *Bulletin of Earthquake Engineering* 19 (12): 5015–5049. https://doi.org/10.1007/s10518-021-01152-7.
Estekanchi, H. E., K. Arjomandi, and A. Vafai. 2008. "Estimating Structural Damage of Steel Moment Frames by Endurance Time Method." *Journal of Constructional Steel Research* 64 (2): 145–155. https://doi.org/10.1016/j.jcsr.2007.05.010.
Eurocode 8. 2005. *European Committee for Standardization, Eurocode 8 (EC8-05): Design of Structures for Earthquake Resistance - Part 3: Assessment and Retrofitting of Buildings*.
Eurocode 8. 2021. *European Committee for Standardization, Eurocode 8(EC8-21): Earthquake Resistance Design of Structures* CEN/TC 250/SC 8:2021.
Falerio, S., S. Oller, and A. Barbat. 2008. "Plastic-Damage Seismic Model for Reinforced Concrete Frames." *Computers and Structures* 86 (7–8): 581–597. https://doi.org/10.1016/j.compstruc.2007.08.007.
Ghobarah, A., H. Abou-Elfath, and A. Biddah. 1999. "Response- Based Damage Assessment of Structures." *Earthquake Engineering and Structural Dynamics* 28 (1): 79–104. https://doi.org/10.1002/(SICI)1096-9845(199901)28:1<79:AID-EQE805>3.0.CO;2-J.
Ghosh, S., D. Datta, and A. A. Katakdhond. 2011. "Estimation of the Park–Ang Damage Index for Planar Multi-Storey Frames Using Equivalent Single-Degree Systems." *Engineering Structures* 33 (9): 2509–2524. https://doi.org/10.1016/j.engstruct.2011.04.023.
Guan, H., and V. Karbhari. 2008. "Improved Damage Detection Method Based on Element Modal Strain Damage Index Using Sparse Measurement." *Journal of Sound and Vibration* 309 (3–5): 465–494. https://doi.org/10.1016/j.jsv.2007.07.060.
Gutiérrez-Urzúa, F., F. Freddi, and L. Di Sarno. 2021. "Comparative Analysis of Code-Based Approaches for Seismic Assessment of Existing Steel Moment-Resisting Frames." *Journal of Constructional Steel Research* 181 (2021): 106589. https://doi.org/10.1016/j.jcsr.2021.106589.
Hancock, J., J. Watson-Lamprey, N. A. Abrahamson, J. J. Bommer, A. Markatis, E. McCoy, and R. Mendis. 2006. "An Improved Method of Matching Response Spectra of Recorded Earthquake Ground Motion Using Wavelets." *Journal of Earthquake Engineering* 10 (I): 67–89. https://doi.org/10.1080/13632460609350629.
HAZUS. 1997. *Earthquake Loss Estimation Method-HAZUS97 Technical Manual*. Washington, D.C: National Institute of Building Sciences.
He, H., S. Cheng, and Y. Chen. 2022. "Earthquake Damage Assessment Model Based on Differential Ratio of Elastic–Plastic Dissipated Energy." *Bulletin of Earthquake Engineering* 20 (5): 2719–2749. https://doi.org/10.1007/s10518-022-01341-y.
Jalayer, F., R. De Risi, and G. Manfredi. 2015. "Bayesian Cloud Analysis: Efficient Structural Fragility Assessment Using Linear Regression." *Bulleting of Earthquake Engineering* 13 (4): 1183–1203. https://doi.org/10.1007/s10518-014-9692-z.
Jalayer, F., P. Franchin, and P. E. Pinto. 2007. "A Scalar Damage Measure for Seismic Reliability Analysis of RC Frames." *Earthq Engineering and Structural Dynamics* 36 (13): 2059–2079. https://doi.org/10.1002/eqe.704.
Krawinkler, H., and A. A. Nassar. 1992. "Seismic Design Based on Ductility and Cumulative Damage Demands and Capacities." In *Nonlinear Seismic Analysis and Design of Reinforced Concrete Buildings*, edited by P. Fajfar and H. Krawinkler, 31–48. Taylor & Francis.

Mibang, D., and S. Choudhury. 2021. "Damage Index Evaluation of Frame-Shear Wall Building Considering Multiple Demand Parameters." *Journal of Building Pathology and Rehabilitation* 6 (1): 40. https://doi.org/10.1007/s41024-021-00134-1.

Mohebi, B., A. H. Chegini, and A. R. Miri Tayefe Fard. 2019. "A New Damage Index for Steel MRFs Based on Incremental Dynamic Analysis." *Journal of Constructional Steel Research* 156 (2): 137–154. https://doi.org/10.1016/j.jcsr.2019.02.005.

Mohsenian, V., R. Filizadeh, and I. Hajirasouliha. 2023. "Seismic Response Estimation and Fragility Curve Development Using an Innovative Response Bound Method." *International Journal of Structural Stability and Dynamics* 23 (20): 2350196. https://doi.org/10.1142/S0219455423501961.

Mohsenian, V., R. Filizadeh, I. Hajirasouliha, and R. Garcia. 2021. "Seismic Performance Assessment of Eccentrically Braced Steel Frames with Energy-Absorbing Links Under Sequential Earthquakes." *Journal of Building Engineering* 33:101576. https://doi.org/10.1016/j.jobe.2020.101576.

Mohsenian, V., R. Filizadeh, Z. Ozdemir, and I. Hajirasouliha. 2020. "Seismic Performance Evaluation of Deficient Steel Moment-Resisting Frames Retrofitted by Vertical Link Elements." *Structures* 26:724–736. https://doi.org/10.1016/j.istruc.2020.04.043.

Mohsenian, V., N. Gharaei-Moghaddam, and A. Arabshahi. 2022. "Evaluation of the Probabilistic Distribution of Statistical Data Used in the Process of Developing Fragility Curves." *International Journal of Steel Structures* 22 (4): 1002–1024. https://doi.org/10.1007/s13296-022-00619-w.

Mohsenian, V., I. Hajirasouliha, and R. Filizadeh. 2023. "Seismic Reliability Assessment of Steel Moment-Resisting Frames Using Bayes Estimators." *Proceedings of the Institution of Civil Engineers - Structures and Buildings* 176 (4): 306–320. https://doi.org/10.1680/jstbu.20.00211.

Mohsenian, V., and A. Mortezaei. 2019. "New Proposed Drift Limit States for Box-Type Structural Systems Considering Local and Global Damage Indices." *Advances in Structural Engineering* 22 (15): 3352–3366. https://doi.org/10.1177/1369433219863299.

Newell, J. D., and C. M. Uang. 2008. "Cyclic Behavior of Steel Wide-Flange Columns Subjected to Large Drift." *Journal of Structural Engineering* 134 (8): 1334–1342. https://doi.org/10.1061/(ASCE)0733-9445(2008)134:8(1334).

Nowak, A. S., and K. R. Collins. 2012. *Reliability of Structures*. 2nd ed. Florida, USA: CRC Press.

Palermo, M., S. Silvestri, and T. Trombetti. 2017. "On the Peak Inter-Storey Drift and Peak Inter-Storey Velocity Profiles for Frame Structures." *Soil Dynamics and Earthquake Engineering* 94:18–34. https://doi.org/10.1016/j.soildyn.2016.12.009.

Park, Y. J., A. H.-S. Ang, and Y. K. Wen. 1987. "Damage Limiting Aseismic Design of Buildings." *Earthquake Spectra* 3 (1): 1–26. https://doi.org/10.1193/1.1585416.

PEER Ground Motion Database, Pacific Earthquake Engineering Research Center. Accessed January, 2021. https://ngawest2.berkeley.edu/.

Powell, G. H., and R. Allahabadi. 1988. "Seismic Damage Prediction by Deterministic Methods: Concepts and Procedures." *Earthquake Engineering and Structural Dynamics* 16 (5): 719–734. https://doi.org/10.1002/eqe.4290160507.

Rodriguez, M. E. 2015. "Evaluation of a Proposed Damage Index for a Set of Earthquakes." *Earthquake Engineering and Structural Dynamics* 44 (8): 1255–1270. https://doi.org/10.1002/eqe.2512.

Rodriguez, M. E. 2018. "Damage Index for Different Structural Systems Subjected to Recorded Earthquake Ground Motions." *Earthquake Spectra* 34 (2): 773–793. https://doi.org/10.1193/021117EQS027M.

Roufaiel, M. S. L., and C. Meyer. 1987. "Reliability of Concrete Frames Damaged by Earthquake." *Journal of Structural Engineering* 113 (3): 445–457. https://doi.org/10.1061/(ASCE)0733-9445(1987)113:3(445).

Smyrou, E., M. J. N. Priestley, and A. J. Carr. 2011. "Modelling of Elastic Damping in Nonlinear Time-History Analyses of Cantilever RC Walls." *Bulletin of Earthquake Engineering* 9 (5): 1559–1578. https://doi.org/10.1007/s10518-011-9286-y.

Sozen, M. A. 1981. *Review of Earthquake Response of Reinforced Concrete Buildings with a View to Drift Control, in State-Of-The-Art in Earthquake Engineering* Edited by O. Ergunay and M. Erdik, 383–418. Ankara, Turkey: Kelaynak Press.

Standard No. 2800. 2014. *Iranian Code of Practice for Seismic Resistant Design of Buildings, Permanent Committee for Revising the Standard 2800*. 4th ed. Tehran, Iran: Building and Housing Research Center.

Tartaglia, R., M. D'Aniello, and R. Landolfo. 2022. "Seismic Performance of Eurocode-Compliant Ductile Steel MRFs." *Earthquake Engineering and Structural Dynamics* 51 (11): 2527–2552. https://doi.org/10.1002/eqe.3672.

Vamvatsikos, D., and C. A. Cornell. 2002. "Incremental Dynamic Analysis." *Earthquake Engineering and Structural Dynamics* 31 (3): 491–514. https://doi.org/10.1002/eqe.141.

Vamvatsikos, D., and C. A. Cornell. 2004. "Applied Incremental Dynamic Analysis." *Earthquake Spectra* 20 (2): 523–553. https://doi.org/10.1193/1.1737737.

Wang, J. F., C. C. Lin, and S. M. Yen. 2007. "A Story Damage Index of Seismically-Excited Buildings Based on Modal Frequency and Mode Shape." *Engineering Structures* 29 (9): 2143–2157. https://doi.org/10.1016/j.engstruct.2006.10.018.

Yang, D., J. Pan, and G. Li. 2010. "Interstory Drift Ratio of Building Structures Subjected to Near-Fault Ground Motions Based on Generalized Drift Spectral Analysis." *Soil Dynamics and Earthquake Engineering* 30 (11): 1182–1197. https://doi.org/10.1016/j.soildyn.2010.04.026.

Zaker Esteghamati, M., M. Banazadeh, and Q. Huang. 2018. "The Effect of Design Drift Limit on the Seismic Performance of RC Dual High-Rise Buildings." *The Structural Design of Tall & Special Buildings* 27 (8): e1464. https://doi.org/10.1002/tal.1464.

Zareian, F., and R. A. Medina. 2010. "A Practical Method for Proper Modeling of Structural Damping in Inelastic Plane Structural Systems." *Computers and Structures* 88 (1–2): 45–53. https://doi.org/10.1016/j.compstruc.2009.08.001.

Zhang, X., K. Wong, and Y. Wang. 2007. "Performance Assessment of Moment Resisting Frames During Earthquakes Based on the Force Analogy Method." *Engineering Structures* 29 (10): 2792–2802. https://doi.org/10.1016/j.engstruct.2007.01.024.

Appendix

Appendix A

This section outlines the process of extracting the probability distribution function of the system response. Additionally, it is explained how in general the desired limit values can be selected. The probability distribution function of inter-story drift at a fixed damage level provides the non-exceedance probability from a desired response value. The following steps detail the extraction of probability distribution curves for the response and the associated interpretation:

(1) Each model undergoes an incremental dynamic analysis (IDA) (see Fig. 6) using a set of records that match the selected site response (20 records introduced in Table 3). In each step of the analysis, the global response of the maximum inter-story drift is determined. Simultaneously, the local responses of the members are evaluated. For each record, once the local response of the members reaches a predefined limit state (e.g. θ_0) for the first time, the corresponding maximum inter-story drift serves as the desired global damage index. It is evident that the result of this step is independent of the intensity parameter utilized in IDA. The resulting data set (Ai) will have the same number of members as the records (Fig. A1(a)).

(2) The statistical set obtained in step 1 (Ai) represents the global damage index associated with a specific local performance level in the frame. According to Fig. A1(b), assuming a log-normal distribution (Mohsenian, Gharaei-Moghaddam, and Arabshahi 2022), the mean (μ) and standard deviation (δ) of the statistical set are calculated. Using Eq. (6) a probability density function in then computed with an unknown parameter for the inter-story drift (f(D)).

$$f(D) = \frac{1}{\sigma\sqrt{2\pi}} \exp\left(-\frac{1}{2} \left(\frac{D-\mu}{\sigma} \right)^2 \right) \tag{6}$$

(3) Determination of probabilities is performed using the EDP-Based method (EDP stands for Engineering Demand Parameter). Accordingly, based on Fig. A1(b) and the mathematical expression in Eq. (7), if D_0 represents an arbitrary global response, the area under the probability density function curve from -∞ to D_0 represents the probability of not achieving that response when the local performance level of the components is θ_0. In technical literature, this probability value (R_0) is known as the non-exceedance probability, and its difference from unity (1) represents the probability of exceeding or fragility (1-R_0) (Mohsenian, Filizadeh, and Hajirasouliha 2023). By varying the values of D_0, the probability distribution of the response at this performance level is extracted. Figure A2(a) depicts the probability distribution of the response along with the concepts of reliability and fragility. As observed in this figure, the probability values are independent of the intensity parameter used in IDA.

$$R = P[(D \le D_0)|(\theta = \theta_0)] = \int_{-\infty}^{D_0} f(D).dD \tag{7}$$

(4) In the final step, for each performance level, the global response values of inter-story drift corresponding to the probability values of 16%, 50%, and 84% (equivalent to μ-δ, μ, and μ+δ) in the probability density function are derived. The average of these obtained values serves as the basis for proposing the performance range (see Table 4).

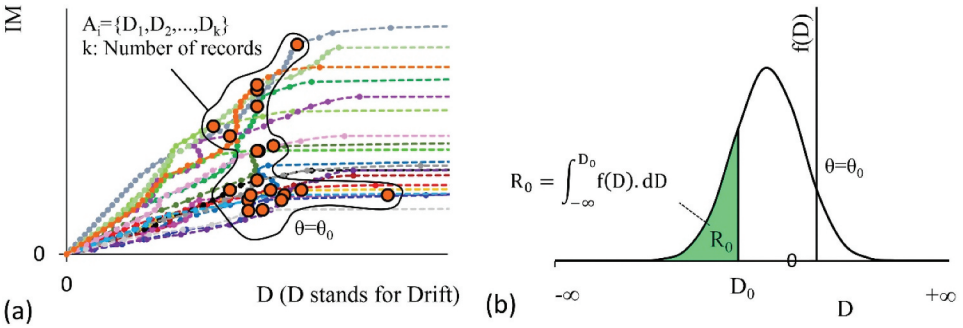

Figure A1. IDA results: (a) The statistical set (Ai) corresponding to the attainment of a local damage level (θ0), and (b) the probability density function associated with the statistical set (Ai) and non-exceedance probability associated with the response of D_0.

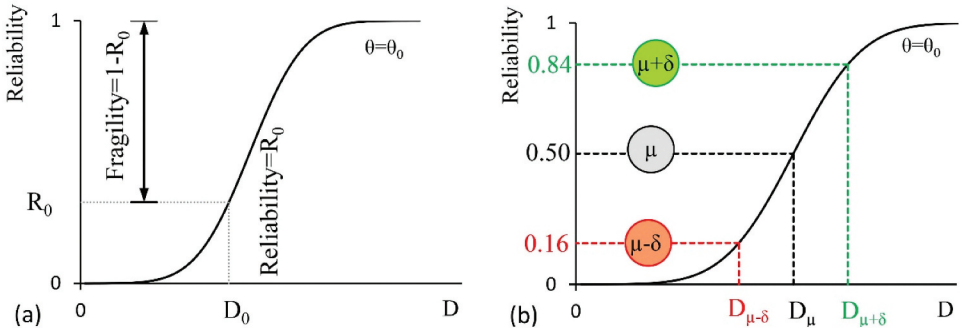

Figure A2. The probability distribution of the global response of maximum inter-story drift when the maximum local response is $θ_0$: (a)reliability curve, and (b) corresponding values to 16%, 50%, and 84%.